POLITECNICO
MILANO 1863

POLITECNICO DI MILANO
MASTER DEGREE IN ENERGY ENGINEERING

PROF. PAILLARD ELIE-ELISEE GEORGES
ELECTROCHEMICAL ENERGY STORAGE DEVICES

INVESTIGATING THE EFFICIENCY AND PERFORMANCE OF NMC-811 LITHIUM-ION BATTERIES WITH GR AND SIC ANODES

Seyed Mohammad Miri Joibary - 10884839

Miguel Cardona Salazar - 10835218

Francesca Agostino - 10868686

Deepak Sundarrajan - 10832614

Marco Lovati - 10628726

ACADEMIC YEAR 2022/2023

Summary

1. Abstract

Batteries are devices that store and release electrical energy through chemical reactions. They are crucial for powering our portable electronics, electric vehicles. Advancements in battery technology will enable greater renewable energy integration, drive the widespread adoption of electric vehicles, support grid-level energy storage, enhance portable electronics, benefit medical applications, and aid aerospace and space exploration. Investing in battery research and development is key to achieving breakthroughs in energy storage technology, leading to improvements in energy density, charging speed, cost reduction, and environmental sustainability.

In the future, battery technology is expected to advance significantly to meet the increasing demand for energy storage. Some are lithium-sulfur (Li-S) batteries, which have the potential for higher energy density. Solid-state batteries, on the other hand, replace the liquid electrolyte in lithium-ion batteries with a solid electrolyte, offering higher energy density, improved safety, and faster charging. Another promising technology is lithium-air (Li-Air) batteries, which utilize oxygen from the air as a reactant and can store several times more energy than lithium-ion batteries.

As for the NMC-811 battery which is Solid-state battery, it is a specific type of lithium-ion battery with a cathode composed of 80% nickel, 10% manganese, and 10% cobalt. NMC-811 batteries offer advantages such as higher energy density, improved stability, and lower cost. However, they also face challenges related to thermal stability and safety.

Our Team has worked on creating these NMC-811 cells using two different types of anodes which are SiC and Graphite electrode. First, we started with the making of half-cell which is the Cathode part of the cells after the building we tested the half-cells to find the efficient ones. Then, we built the two types of anodes for the cells which are made by SIC and Graphite. These two types of NMC-811 batteries are then tested to find the efficient one among them. From, our results we can find that the graphite anode NMC-811 are better than the SIC NMC cells which we found by comparing the columbic efficiency of these cells which will be explained in detail in the report.

2. Introduction

A battery is a device that stores chemical energy and converts it to electrical energy. The chemical reactions in a battery involve the flow of electrons from one material (electrode) to another, through an external circuit. The flow of electrons provides an electric current that can be used to do work. To balance the flow of electrons, charged ions also flow through an electrolyte solution that is in contact with both electrodes. Different electrodes and electrolytes produce different chemical reactions that affect how the battery works, how much energy it can store and its voltage.

NMC batteries are made up of Nickel, Manganese, Cobalt in various ratios. The NMC batteries are also called as ternary batteries, which means batteries made up of three materials. NMC 811 battery is an upgrade on the existing battery in the market which is NMC-622. The NMC-811 battery has a slight upgrade on specific capacity of the battery which would be 12% more than NMC-622. This foundation is composed of the mainstream lithium battery, in accordance with the different dosage ratios of nickel, cobalt and manganese materials of the battery cathode. Other than these there are various models such as 111 type, 523 type, 622 type and 811 type, etc.

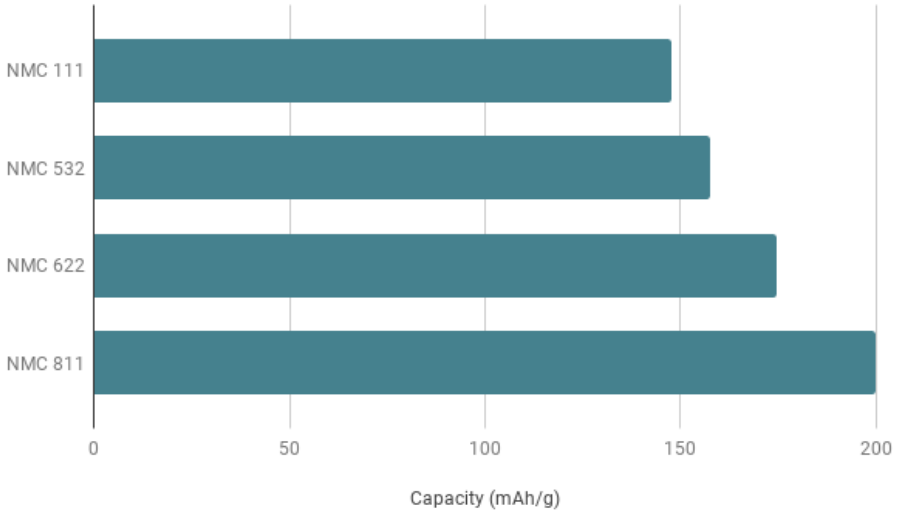

Figure 2.1 - Capacities of various NMC Batteries

To date, batteries with NMC chemistry remain the most frequently used in the automotive sector.

With this chemistry, a very high specific energy of up to 220 – 240 Wh/kg can be achieved. This is clearly a decisive competitive advantage for a car, as it allows a large amount of energy to be stored with a low weight and volume, allowing more energy to be installed in the vehicle than other lithium-based technologies.

The most significant feature of the NMC 811 battery is its high energy density. This comes from the **nickel** in the cathode which can increase the material activity and thus the energy density. Plus, the high nickel content is important for increasing the capacity. The **cobalt** is also an active component that stabilizes the laminar structure of the material, thereby increasing the discharge capacity of the material. The **manganese** component, which plays a supporting role in the electrodes, provides stability during charging and discharging. For example, Grepow's NMC 811 battery has an energy density of 275 Wh/Kg.

NMC 811s are the newest: they have a high nickel concentration and a very low manganese and cobalt content. This results in higher energy density at a lower cost. It is therefore clear that NMC technology, in its evolution, has likewise set itself the ambitious goal of reducing cobalt as much as possible, but this is still a very laborious process, because cobalt is an element that gives stability to the system and increases life cycles. Research does not stop, however; on the contrary, there are already companies experimenting with innovative new technologies in this respect, such as Svolt for example, which recently announced the first NMX cell, completely free of cobalt.

These batteries are used in various electronic devices such as:

- Power tools
- Electric power trains
- Electric bikes
- Drones
- Laptops
- Solar Storage

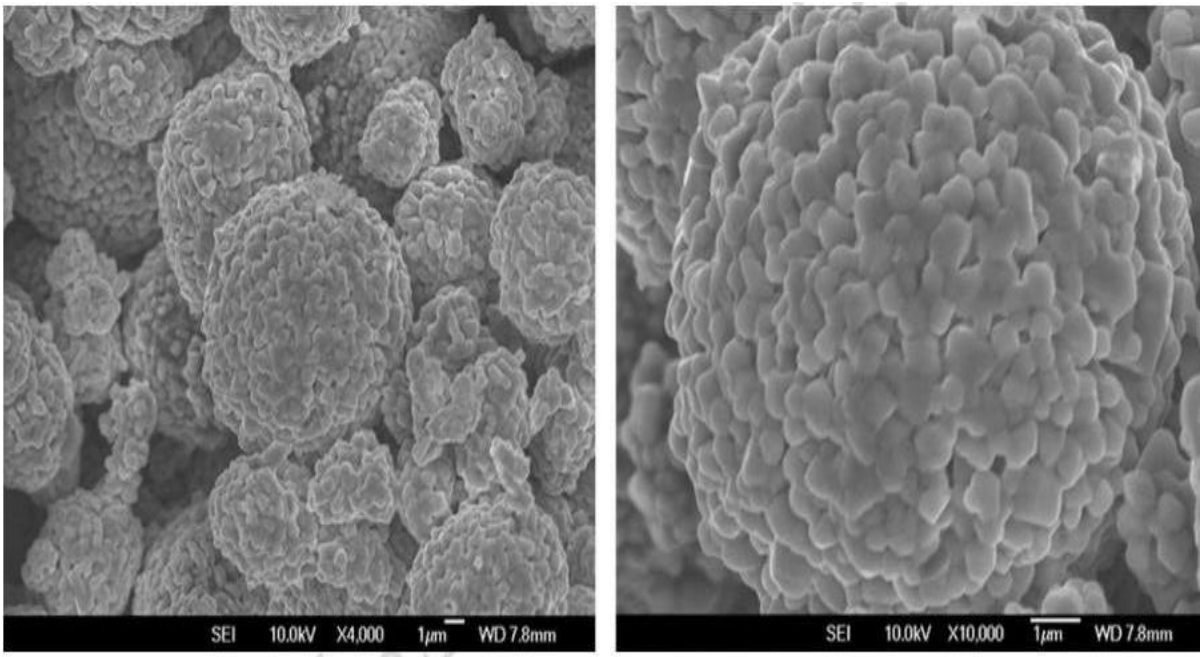

Figure 2.2 Microscopic image of cathode (1)

The image above shows how the NMC-811 which is the cathode part of the cell looks in microscopic image. NMC-811 would appear as a fine powder consisting of tiny particles with varying sizes and shapes. These particles would typically have a spherical or irregular shape, and their color would depend on the specific manufacturing process and any surface coatings applied. The image might show a cluster of particles with visible boundaries between them, indicating the group of NMC-811 particles. Additionally, the surface of the particles might display a rough or textured texture, suggesting the presence of nanostructured or porous features.

3. Cathode

We will move on to the procedure of creating the new cell and analysis it, which involves creating a cathode and anode of the cell. We start with creating the cathode of the NMC-811 cell as the first part. After preparing the cathode we will run it for testing to pick the efficient one. Then we will go on to prepare the anode for the cell.
In this section we analyze the practical application for the cathode.

3.1 Materials

First, we design a cathode sheet with a known composition. For the active material cathode, we use:

- NMC811: $LiNi_xMn_yCo_zO_2$ $(x + y + z = 1)$, in the current case x= 0.8, y= 0.1 and z=0.1.
- PVDF: stands for Polyvinylidene Fluoride. It is a polymer material used as a binder to hold the materials together. It´s known for its excellent chemical resistance, high thermal stability, and electrical insulation properties.
- Conductive carbon (Super P): is a brand name for a specific type of carbon black powder used in various industries and applications. Carbon black is a form of elemental carbon produced by the incomplete combustion of hydrocarbons. It consists of fine particles that are predominantly composed of carbon.
- NMP: stands for N-Methyl-2-pyrrolidone. It is a common organic compound that belongs to the class of solvents known as pyrrolidines. NMP is a colorless liquid with a high boiling point and low volatility. It was used as a solvent for mixing all the components of the cathode slurry.

These components are weighed in an electrode balance with accuracy up to 0.1 mg.

Sl. No.	Materials for Cathode	Theoretical weight of each Ingredient	Real weight of each Ingredient
01	$LiFePO_4$ (Lithium Iron Phosphate)	0.6 g	0.6096 g
02	PVDF (Polyvinylidene fluoride)	0.075 g	0.0762 g
03	Super P (structured carbon black powder)	0.075 g	0.0762 g
04	NMP (N-Methylpyrrolidone)	0.1953 g	0.2036 g

Table 3.1 - Components for half cell.

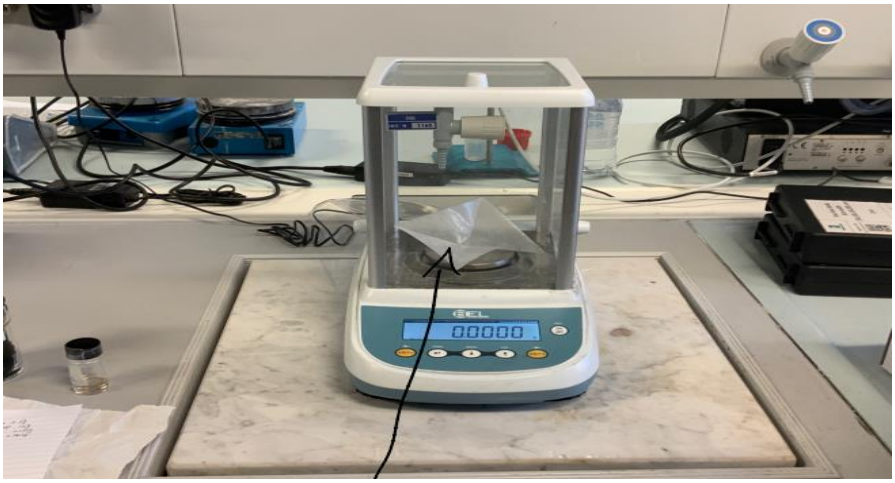

Figure 3.1 - Balance to weigh our materials

First, we weight the PVDF, then we added the other ingredients from table 1 to the ceramic container, that was going to be used to hold the slurry during the ball milling process.

3.2 Procedure

During the ball milling process, the objective was to homogenize the slurry components and ensure proper dispersion of their constituents, including the breaking of agglomerates created by the adherence of adjacent particles. The zirconia spheres used in the ball mill had the benefit counting with a high tenacity among the ceramic materials, which prevents the fracturing and contamination ZrO_2 into the composition of the slurry.

During the mixing process, the slurry together with the zirconia spheres was placed in a sealed ceramic container, avoiding the spillage of the content, or the introduction of impurities from the ambient. The mixing speed was set to 100 RPM for 30 minutes, then the speed was increased from

100 to 250 RPM, and the duration from 30 minutes to 1 hour in one sense of rotation, and another hour in the opposite sense.

Figure 3.2 – Planetary ball mill

In the meantime, an aluminum sheet which acts as a current collector and substrate for the cathode material for mechanical stability, is to be cleaned by isopropanol to remove dirt or residue. The sheet will have two sides, one side with a glossy surface and the other with a rough one. Each surface is cleaned and left to dry for 30 minutes.

After this period, the container is retrieved, and any excess material adhering to the balls is collected and applied onto aluminum foil to ensure even distribution. A cylindrical roller of 80-90 mm with a consistent diameter and a clearance gap of 100 microns is used to achieve the desired thickness of LiFePO4 over the aluminum foil.

Figure 3.3 – Cylindrical roller

Figure 3.4 – Active material on the aluminum foil

The foil is kept for drying in oven at 80°C for few days after which it is cut into circular shape and pressed at load of 3 tons. At this load the thickness of foil is reduced to 26 microns from 33 microns approximately. The cathode was reduced because it must be smaller than the anode otherwise, we would have accumulation of lithium in the cathode side. We must get at least eight cuts from foil without any wrinkles or folds over the surface. We cut 9 small cathode disks with a diameter of 12 mm, and we weigh them with the electrode balance. We repeated these steps for the 10 circular shape disks of pure aluminum, but this time we weighed all the disks together, resulting 0.048 g. (*see figures 3.5 and 3.6*).

Figure 3.5 - Press to make disks

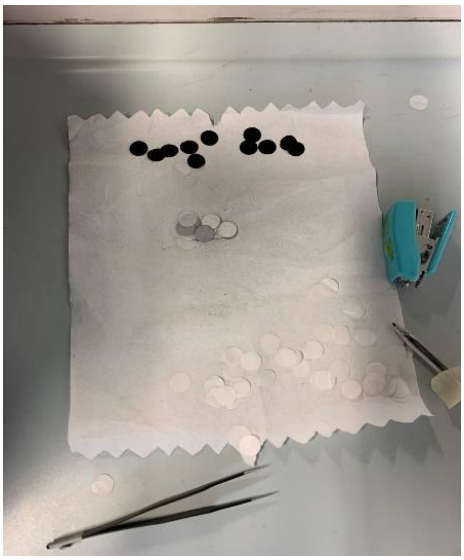

Figure 3.6 - Disks of active material

Trial No.	1	2	3	4	5	6	7	8	9
Weight (g)	0.0075	0.0069	0.0075	0.0076	0.0076	0.0077	0.0074	0.0072	0.0072

Table 3.1 – Weight of active material disks

4. Half Cell

Now we are ready to assemble our active material with other components to make the half cell. The half-cell allow us to investigate one of the half reactions that occurs in the Li-ion cell(in our case the cathode reaction). Just one electrode will be used and a Li foil is used as the counter electrode(anode). It's important to note that a half-cell is a simplified representation used for studying and understanding individual electrode reactions.

4.1 Materials and Instruments

We have built different half coin cells (or button cell battery) that are composed by cathode case, cathode, separator with electrolyte, lithium foil, spacer, spring and anode case.

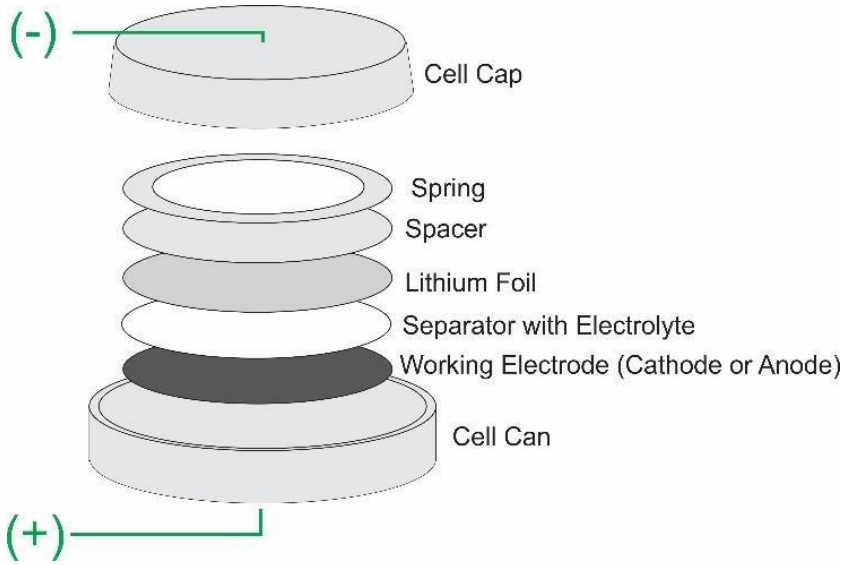

Figure 4.1 – Half-cell structure (2)

The **cathode case** serves as the housing for the cathode electrode and provides several important functions:

- Enclosure: The cathode case encloses the cathode electrode and protects it from physical damage, contamination, and external influences. It provides secure and protective housing for the cathode component of the battery.
- Electrical Isolation: The cathode case is designed to electrically isolate the cathode electrode from the anode electrode, which may be housed in a separate container or compartment in the

complete button cell configuration. This prevents direct electrical contact between the two electrodes, ensuring the proper functioning of the half-cell configuration.

- Connection Point: The cathode case often serves as the connection point for the external circuit. It provides a terminal or contact point where an external device or circuit can be connected to draw or supply electrical current. The cathode case establishes the electrical connection between the cathode electrode and the external circuit.
- Structural Support: The cathode case provides structural support to the overall battery. It helps maintain the integrity of the battery cell and keeps the components properly aligned. It ensures that the cathode electrode is securely held in place within the battery assembly.

The **cathode** (positive electrode) plays a crucial role in the electrochemical reaction. The main function of the cathode in a half-cell battery is to facilitate the reduction half-reaction.
In the half-cell configuration, the cathode electrode is typically made of a material that can accept electrons and undergo reduction. When the battery is connected in a circuit, the cathode attracts the electrons released by the anode (negative electrode) in the other half-cell.
In discharge the reduction half-reaction at the cathode involves the acceptance of electrons and the incorporation of lithium ions into the cathode material (reduction reaction). The specific cathode material determines the voltage, energy density, and other characteristics of the button cell battery. The reduction reaction occurring at the cathode is complemented by the oxidation half-reaction at the anode, completing the electrochemical process and enabling the flow of electrons through the external circuit. The electrode prepared in the lab which is made of NMC811.

The **separator** is a thin, porous material that physically separates the cathode and anode of the battery. Its primary function is to prevent direct contact between the cathode and anode, which could cause a short circuit and potentially lead to battery failure or safety hazards.
The separator is typically made of a non-conductive material, often a porous polymer or a microporous membrane. In our case it is made of a glass fiber. It allows for the passage of ions while inhibiting the flow of electrons (thanks to the electrolyte in which it´s soaked, this will be deepen ahead). This selective permeability enables the movement of ions between the cathode and anode

during the electrochemical reactions, while preventing the direct flow of electrons that could cause a short circuit.
The separator's porous structure allows for the transport of electrolyte ions, such as lithium ions in a lithium-based button cell battery, while minimizing the risk of internal short circuits. By maintaining the physical separation between the cathode and anode, the separator helps to maintain the battery's stability, integrity, and overall performance. In addition to its role in preventing short circuits, the separator may also provide other functions such as absorbing excess electrolyte, helping to maintain the battery's internal pressure, and contributing to the overall mechanical structure of the battery.

The **electrolyte** is a substance or solution that acts as a conductor of ions between the cathode and anode. It facilitates the movement of ions during the electrochemical reactions that occur within the battery.
In most button cell batteries, the electrolyte is a liquid or gel-like substance that contains ions, typically in the form of a salt dissolved in a solvent. The choice of electrolyte depends on the specific battery chemistry. Here we used LiPF6 in an EC/DMC solution. The electrolyte not only provides a medium for ion conduction but also contributes to the overall performance and safety of the battery. It should have good ionic conductivity, low resistance, and good compatibility with the cathode, anode, and separator materials, plus preventing parasitic side reactions (e.g H_20 electrolysis). The choice of electrolyte is crucial in determining the battery's voltage, capacity, internal resistance, and overall electrochemical behavior.

The **spacer** is a component used to fill the empty space inside the battery case and provide proper fit and stability for the various internal elements. It ensures that the electrode stack, separator, and other components remain properly aligned and positioned within the battery. Spacers are typically made of insulating materials and help maintain the structural integrity of the battery.

The **spring** is a component that provides contact between the battery and the external device or circuit. It is typically located on the negative terminal side of the battery.
The spring is designed to provide a secure and reliable connection. Its purpose is to maintain continuous electrical contact between the battery and the device it powers. The spring in a button cell battery is often compressed when the battery is inserted into a device or battery holder. The

compression of the spring creates pressure against the battery, ensuring a firm connection and minimizing the risk of intermittent or loose contact.
By establishing a solid electrical connection, the spring allows the flow of electrons from the battery to the external circuit, enabling the battery to power the connected device or circuit.

The **lithium foil** serves as the anode (negative electrode) of the button cell battery. A half-cell is a simplified representation of a battery where only one electrode is present, allowing for the study of individual electrode reactions. The active material in the half cell assembly is Lithium metal. For commercial uses, graphite is commonly used, to reach its final lithiated form of LiC_6.
The main function of the lithium foil in a half-cell button cell battery is to provide a source of lithium ions for the electrochemical reaction. When the battery is connected to a complete circuit, the lithium atoms in the lithium foil undergo oxidation, releasing lithium ions (Li^+) into the electrolyte solution. In this configuration, the half-cell with the lithium foil represents the anode side, where the oxidation half-reaction occurs:

$$Li(s) \rightarrow Li^+ + e^-$$

This reaction involves the conversion of solid lithium (Li) into lithium ions (Li+), with the release of an electron (e-). The released lithium ions then migrate through the electrolyte to the other electrode (cathode) in the battery, where a corresponding reduction half-reaction takes place.

The assembly of the half cells must be done in a controlled environment to protect sensitive materials from exposure to air and moisture, ensuring their stability and integrity during manipulation or experimentation. This is the **vacuum glove box** that provides with low levels of oxygen and moisture, typically achieved by creating a vacuum or purging with inert gases such as nitrogen or argon.
The vacuum glove box consists of a sealed chamber or enclosure that is transparent, allowing users to view and manipulate the contents inside. The enclosure is typically made of durable materials like stainless steel or acrylic to maintain airtightness.

Figure 4.2 - Vacuum glove box

The primary purpose of a vacuum glove box is to provide a controlled atmosphere free of oxygen and moisture, which can degrade or react with sensitive materials, such as chemicals, reactive metals, or certain biological samples. The controlled environment helps to preserve the integrity and stability of these materials during handling, processing, or experimentation.

The glove box is equipped with built-in gloves attached to sealed ports, allowing operators to handle and manipulate objects inside the enclosure without breaking the controlled atmosphere. These gloves are typically made of materials like butyl rubber or neoprene, which offer excellent resistance to oxygen and moisture permeation.

Vacuum glove boxes often include various features and accessories to enhance usability and functionality, such as gas purifiers or scrubbers to maintain the desired atmosphere, pressure control systems, temperature control, and sometimes integrated tools like vacuum pumps or humidity monitors.

In a half-cell configuration of a button cell battery, the term "**anode case**" is not commonly used or applicable. In a half-cell setup, only one electrode (either the anode or the cathode) is present, and the focus is on studying the individual electrode reaction.

However, in a complete button cell battery, which comprises both the anode and cathode, as well as other components, an anode case may be present and has the same function of cathode case.

Firstly, the assembly start's with placing the cathode active material inside the cathode case, care must be taken such that the active material should not touch corners of the case and must be placed as closer to the center as possible. This step is followed by placing a separator over cathode active material but this time as soon as the separator is placed, electrolyte is added in the cathode case. Finally, lithium metal is added to case and even here, the lithium layer should not touch the case. Now, the anode case is covered along with spring and spacer. This cell is sealed in an equipment by applying 1 ton load. After sealing, another cleaning process is carried out to eliminate any remaining excess electrolyte. Finally, the coin cell is removed from the vacuum glove box for testing purposes.

Figure 4.3 – Press in the vacuum glove box

5. Full cell

At this point, we have the aim to assemble our full cell.
A coin cell is a type of small, cylindrical battery that is commonly used in various electronic devices. It is named "coin cell" because is typically thin and round, resembling the shape and size of a coin. Their size ranges from 5 to 25 millimeters in diameter and 1 to 6 millimeters in height. Coin cells are widely used due to their compact size, ease of use, and long shelf life. They are often used in devices that require a low amount of power, such as calculators, watches, remote controls, small electronic toys, and medical devices. They are also commonly used in backup power applications, memory retention, and as power sources for real-time clocks in electronic systems.

While the half-cell refers to one of the two electrodes in an electrochemical cell, the full cell presents both the anode and the cathode. The two half cells work together to create a complete electrochemical system where electrons flow from the anode to the cathode, allowing the redox reaction to occur.
We have built 4 different full cells. Each of them is composed by cathode case, cathode, separator with electrolyte, a layer of metal, anode, spacer, spring and anode case.

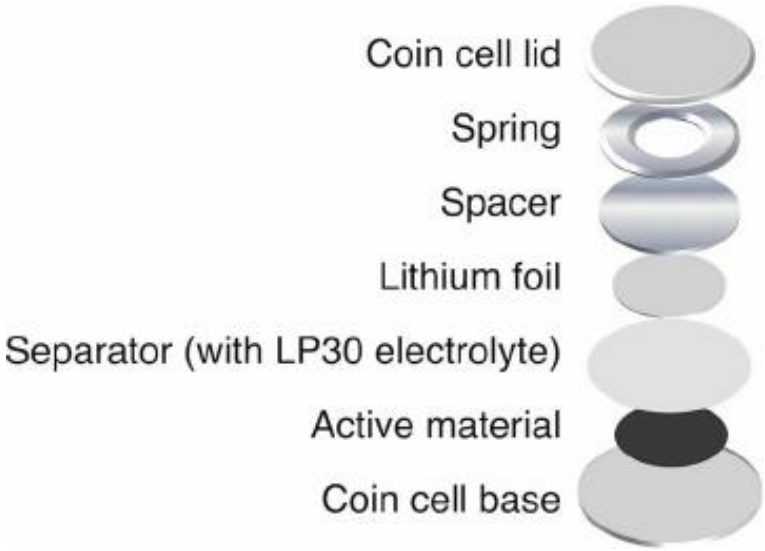

Figure 5.1 – Full cell structure (2)

The cathode for these cells is NMC811 while for anode we use Graphite or SiC.

In this table we have the composition of our 4 cells, chosen coupling cells that have similar aerial capacity:

	Anode		Cathode	
# of cell	**Composition**	**Aerial Capacity (mAh/cm2)**	**Composition**	**Aerial Capacity (mAh/cm2)**
Cell1	Graphite	0.300594731	NMC 811	0.288849558
Cell2	Graphite	0.300594731	NMC 811	0.311504425
Cell3	SiC	0.313571779	NMC 811	0.300176991
Cell4	SiC	0.253269513	NMC 811	0.220884956

Table 5.1 - Coupling between anode and cathode for full cell

The procedure and components to assemble the full cell is almost the same as that of half-cell. The only difference now is the presence of the anode and a layer of metal.

The **anode** plays a critical role in the overall function of the battery. It refers to the electrode that acts as the negative terminal of the battery. It is the electrode where oxidation reactions occur during the discharge process. The anode is typically made of a material that can accept and release ions.

For 2 of the 4 cells, we use Gr (graphite) as anode. It is a common material used for anodes in button cell batteries. So, the function of a graphite anode in a button cell battery is to provide a stable and efficient electrode for the electrochemical reactions that occur during battery operation.
For the last 2 cells we use SiC (silicon + conductive carbon) as anode. It is not a commonly used material for anodes in button cell batteries. The anode's primary role is to provide a site for oxidation or release of electrons during the electrochemical reactions that occur within the battery.
In the case of SiC as an anode material, it would be expected to undergo oxidation when the battery is in use.

The assembly of the full cells like half cells must be done in a controlled environment to protect sensitive materials from exposure to air and moisture, ensuring their stability and integrity during manipulation or experimentation. In full cell assembly, we place the **layer of metal** after the

electrolyte. In this case the anode is thinner, the compression of the metal creates pressure against the battery prevents the anode from moving.

Here, the assembly procedure takes place in the vacuum glove box and as previously reported, the steps are the same as for the half cells.

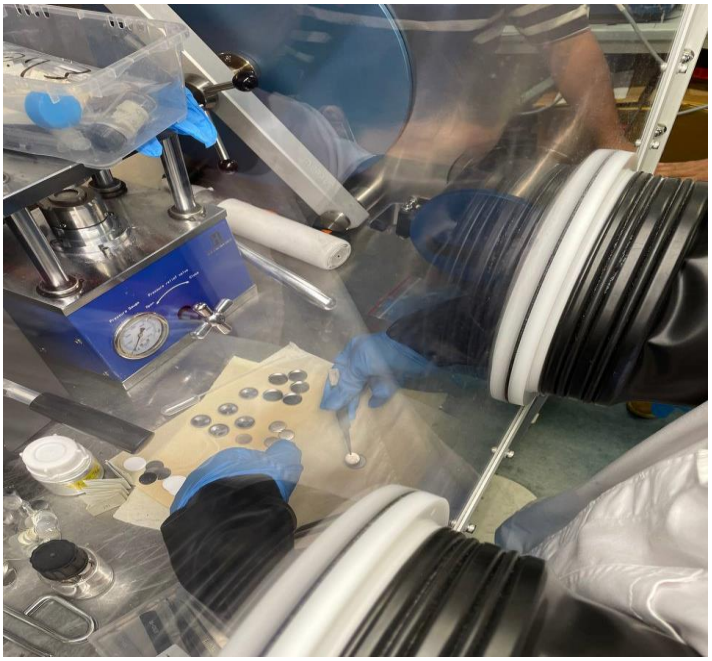

Figure 5.2 – Cell assembly

6. Results of Half Cell and Full Cell

To evaluate the electrochemical performance of the coin cell battery system, we conducted tests on both half cells and full cells. These tests were carried out to assess the individual electrode materials in isolation (half cells) as well as the overall performance of the assembled coin cell battery system (full cells). The following subsections outline the methodologies employed and the results obtained from each test.

Neware is a well-known brand that specializes in manufacturing battery testing systems and equipment. Their battery testing systems are designed to accurately measure and analyze the performance of various types of batteries. In our test step we use Neware's battery testing systems for our work.

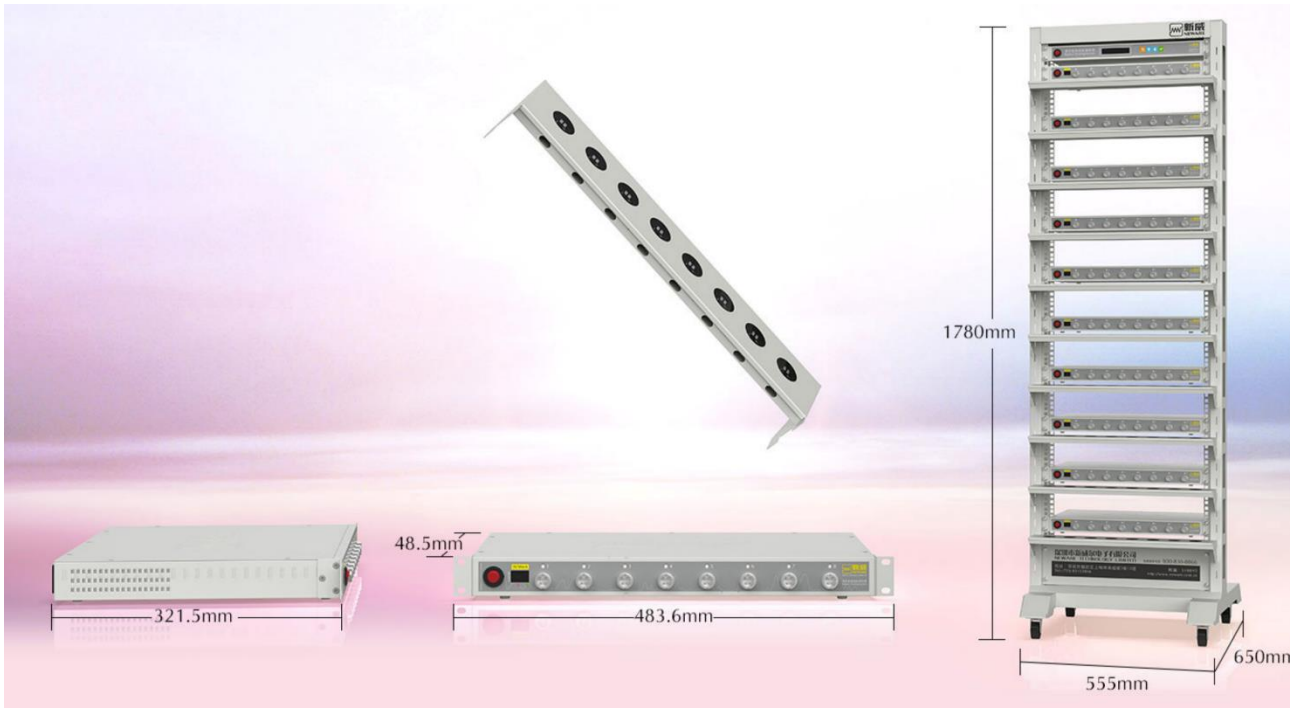

Figure 6.1 – Structure of Neware's battery testing systems (3)

Neware's battery testing systems typically consist of a hardware device, such as a battery cycler, and accompanying software for data analysis. The hardware device is responsible for applying specific

charge and discharge cycles to the battery under test, while the software is used to collect and analyze the data generated during the testing process.

The data analysis capabilities of Neware's testing system software allow users to extract valuable insights and metrics from the battery testing results. Here are some key aspects of Neware's data analysis features:

1. **Voltage and Current Analysis**: The software provides detailed information about the voltage and current profiles during charge and discharge cycles. Users can analyze these profiles to understand the battery's performance characteristics, such as voltage sag, capacity loss, and efficiency.
2. **Capacity and Energy Analysis**: Neware's software allows users to calculate and analyze the battery's capacity and energy metrics. This includes measurements such as initial capacity, capacity fade over time, energy efficiency, and coulombic efficiency. These metrics are crucial for assessing the battery's performance and determining its cycle life.
3. **Resistance Analysis**: The software enables users to evaluate the battery's internal resistance. By analyzing the resistance measurements, users can gain insights into the battery's impedance behavior, which impacts its power output, heat dissipation, and overall performance.
4. **Cycle Life Analysis**: Neware's software provides tools for analyzing the battery's cycle life, which refers to its ability to endure repeated charge and discharge cycles. Users can track the battery's capacity retention over time, estimate its cycle life expectancy, and identify any degradation patterns or failure modes.
5. **Data Visualization and Reporting**: The software offers visualization tools to represent the test data in the form of graphs, charts, and tables. These visual representations make it easier to interpret the results and communicate them effectively. Additionally, Neware's software often includes reporting capabilities, allowing users to generate comprehensive test reports summarizing the key findings.

Overall, Neware's battery testing system and data analysis software provide a comprehensive solution for characterizing and understanding battery performance. The combination of hardware testing capabilities and advanced data analysis features enables users to make informed decisions regarding

battery selection, optimization, and quality control in various applications, such as electric vehicles, energy storage systems, and portable electronics.

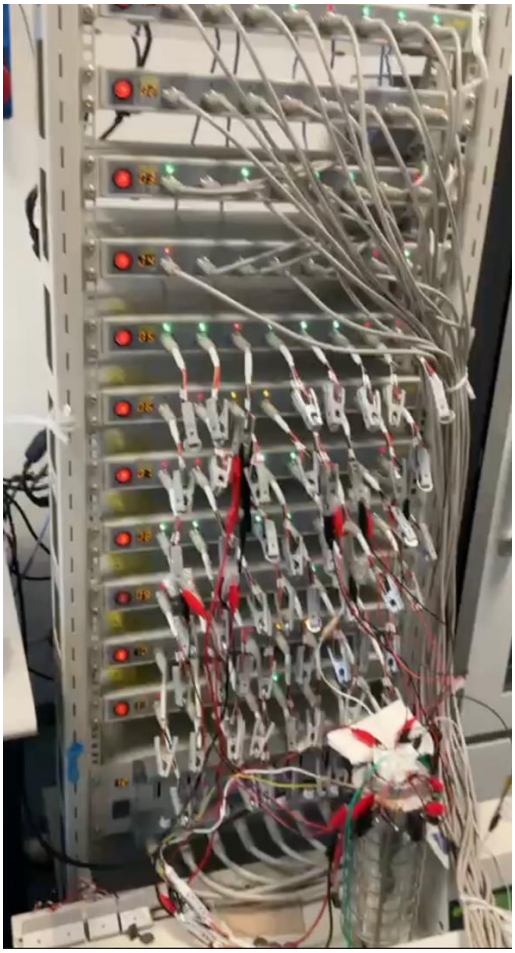

Figure 6.2 - Structure of Neware's battery testing systems and other connections in lab

6.1 Half Cell testing

To investigate the electrochemical behavior of the individual electrode materials, half cells were fabricated using NMC811 as the cathode material and lithium foil as the anode material. The electrolyte used was LiPF6 in an EC/DMC solution.

The half-cell testing involved cyclic voltammetry (CV) and galvanostatic charge-discharge (GCD) techniques. In CV, the potential of the NMC811 cathode was swept over a specified range at a constant scan rate to observe the redox reactions and capacitive behavior. The lithium foil anode acted as a reference electrode. GCD involved applying a constant current to the NMC811 cathode and monitoring the resulting voltage response over time.

The obtained CV curves provided information about the redox processes occurring at the NMC811 cathode/electrolyte interface, while the GCD profiles gave insights into the charge storage capacity and stability of NMC811. By comparing the half-cell performance of NMC811 with lithium foil as the anode, we were able to assess the compatibility and performance of this electrode combination.

The nominal capacity calculation requires the cell diameter (13 mm) and the cell area (1.32 cm^2). We choose a practical capacity of active material equal to 0.18 which corresponds to 180 mA/g_{ac}. The calculation is done in the following way:

$$C_n = 180\left(\frac{mAh}{g_{ac}}\right) \cdot 2.810 \cdot 10^{-3}(g_{ac}) = 0.504\, mAh$$

Where $2.810 \cdot 10^{-3}$ is the weight of active material. It results that the nominal capacity is equal to 0.000504 A, and it depends on the active material of the single cell, so it varies. However, the software does not have enough significant digits, so the nominal capacity is the same for all the cells.

Cell No.	Std.C-Rate	Weight of the cells (g)	Weight of the al(g)	80% capacity(mAh)	Nominalcapacity (mAh)
1	180	0.0075	0.0048	0.8	0.3888
2	180	0.0069	0.0048	0.8	0.3024
3	180	0.0075	0.0048	0.8	0.3888
4	180	0.0076	0.0048	0.8	0.4032
5	180	0.0076	0.0048	0.8	0.4032
6	180	0.0077	0.0048	0.8	0.4176
7	180	0.0074	0.0048	0.8	0.3744
8	180	0.0072	0.0048	0.8	0.3456
9	180	0.0072	0.0048	0.8	0.3456

Table 6.1 - Technical values for cells.

In the test procedure we increase the C-rate in the various cycles for practical reasons, otherwise the test would last weeks. The test procedure for the cells 1,3 and 4 are the following:

Cycle ID 1-2-3-4		Cycle ID 5-6-7		Cycle ID 8-9-10		Cycle ID 11-12-13	
mode	C-rate	mode	C-rate	mode	C-rate	mode	C-rate
CC Chg	0.1	CC Chg	0.3	CC Chg	0.5	CC Chg	1
CV Chg	0.05	CC DChg	0.3	CC DChg	0.5	CC DChg	1
CC DChg	0.1						

Cycle ID 14-15-16		Cycle ID 17-18-19		Cycle ID 20-21-22		Cycle ID 23:74	
mode	C-rate	mode	C-rate	mode	C-rate	mode	C-rate
CC Chg	2	CC Chg	3	CC Chg	5	CC Chg	1
CC DChg	2	CC DChg	3	CC DChg	5	CC DChg	1

Table 6.3 – Testing procedure cells 1,3 and 4

The cells 5,6 and 7 are tested using the same procedure but in a different channel:

Cycle ID 1-2-3		Cycle ID 4-5-6		Cycle ID 7-8-9		Cycle ID 10-11-12	
mode	C-rate	mode	C-rate	mode	C-rate	mode	C-rate
CC Chg	0.2	CC Chg	0.3	CC Chg	0.5	CC Chg	1
CC DChg	0.2	CC DChg	0.3	CC DChg	0.5	CC DChg	1
Cycle ID 13-14-15		Cycle ID 16-17-18		Cycle ID 19-20-21		Cycle ID 22:73	
mode	C-rate	mode	C-rate	mode	C-rate	mode	C-rate
CC Chg	2	CC Chg	3	CC Chg	5	CC Chg	1
CC DChg	2	CC DChg	3	CC DChg	5	CC DChg	1

Table 6.4 – Testing procedure cells 5,6 and 7

6.1.1 Cell failures

After the test we noticed a strange behavior in cells 4 and 7 as reported in figures below.

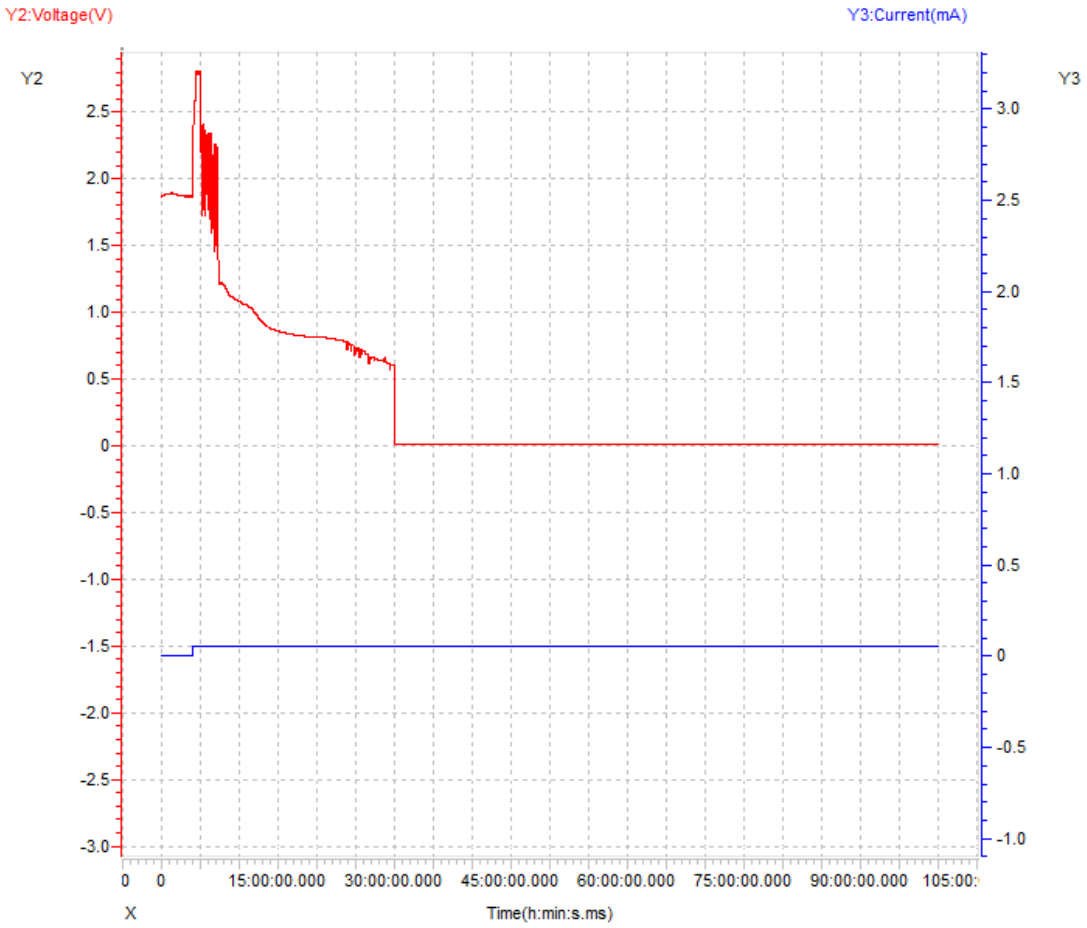

Figure 6.3 – Voltage – current - time graph of cell 4

Analyzing the Voltage and current of the cell in time we can notice a failure of the cell after the first cycles.

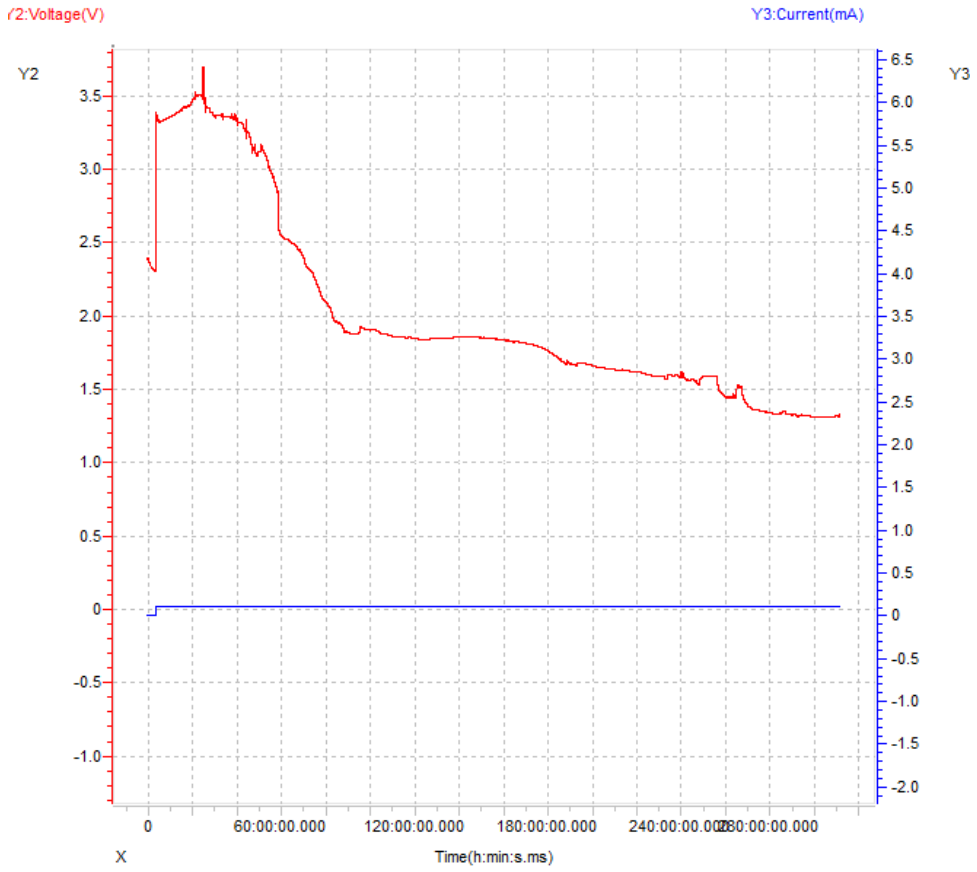

Figure 6.4 - Voltage – current - time graph of cell 7

Also the cell 7 has a failure after the first cycles we can assume a short circuit due to dendrites occurred but we can't have the certain cause because we didn't do a postmortem analysis.
Therefore, it's evident that cells 4 and 7 are useless for our analysis so we decided to neglect these two cells.

6.1.2 Voltage vs capacity profile

The relationship between voltage and capacity in a button cell battery can be influenced by various factors, including the battery chemistry, discharge rate, and state of charge. Generally, the voltage of a button cell battery remains relatively stable during most of its discharge cycle until it approaches the end of its life. In a discharged state, the voltage of a button cell battery is typically lower. As the battery is charged, the voltage increases until it reaches its fully charged state. The voltage during charging is usually higher than the voltage during discharge.

Regarding capacity, it is important to understand that capacity and voltage are not directly proportional in a button cell battery. The capacity of a battery refers to the amount of charge it can store, typically expressed in milliampere-hours (mAh). On the other hand, voltage represents the electrical potential difference between the battery's positive and negative terminals.
While the capacity of a battery indicates the amount of charge it can deliver over a specific period, the voltage remains relatively constant until the battery is depleted. As the battery discharges, the voltage gradually decreases, indicating that the available charge is being consumed.

First, we analyze the voltage profile of **cell 1**.

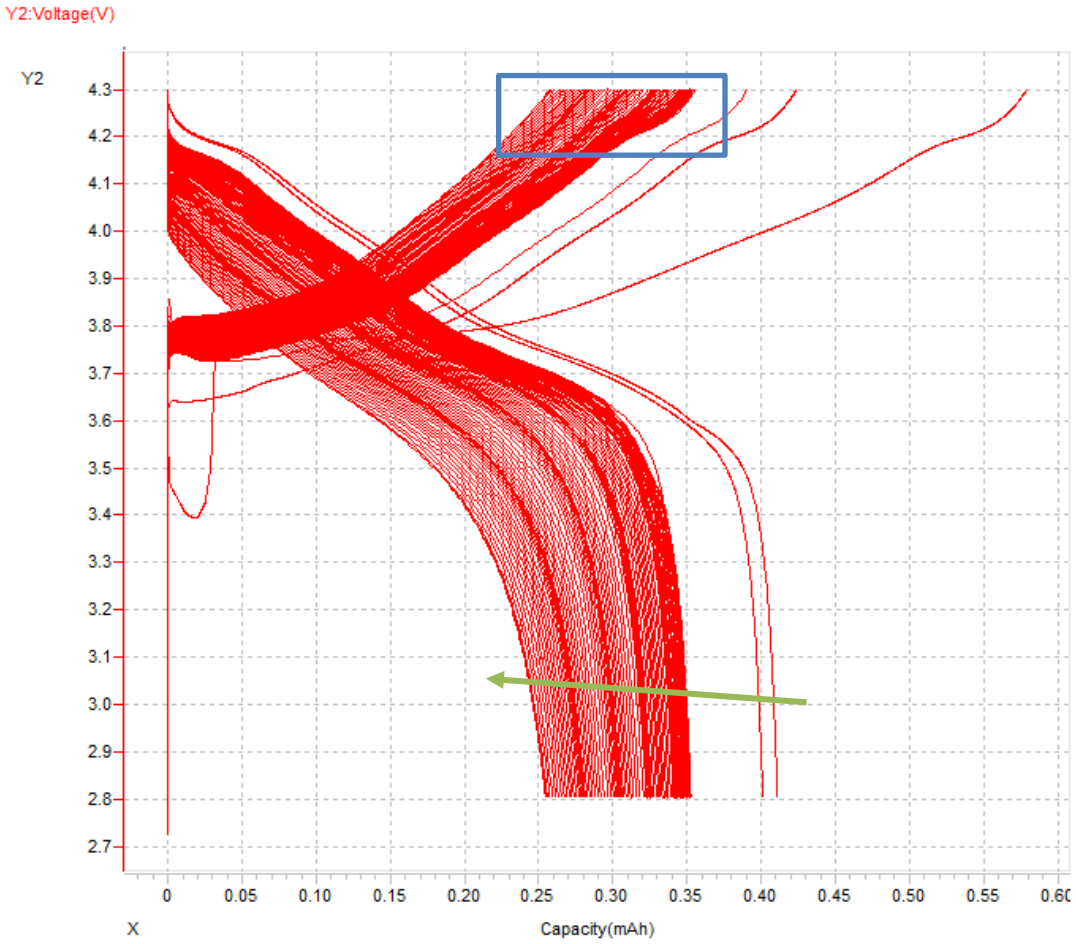

Figure 6.5 – Voltage vs capacity profile cell 1

Historically, in different projects, the cyclability of NMC at high Ni loadings, has encountered issues, leading in some cases to the oxidation of the electrolyte. There are also other hypothesis for this

plateau, which will be exposed below. We can see a decay in the last part of the Discharge curve caused by the cycling. The decay is not always uniform (i.e later cycles have larger "jumps" in the capacity fading).

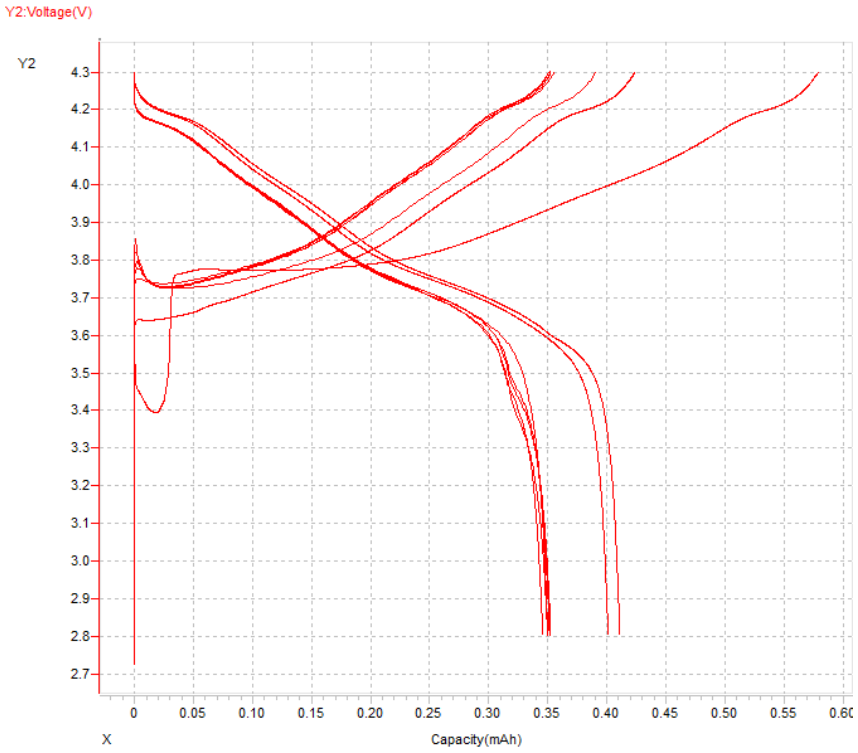

Figure 6.6 - Voltage vs capacity profile, cycles 1-7 cell 1

Highest capacity for first charging, followed by a rapid decay in the first 7 cycles. In the first cycle we have a strange decay of the voltage at low capacity but it's normal for our cathode.
An additional capacity fade mechanism of this material might be. This layered material presents the conditions that Ni (+2) has a similar size in comparison to Li (+1), hence some Li can replace Ni (+2) leading to an issue due to ever-increasing blocked Li^+ to take part of the charge transfer in the case of the halve cell, and in the full cell, where lithium is scarcer than in the halve cell with a Li/metal anode, it can directly impact the active material participating in the redox reaction (4).

Now we analyze the Voltage profile of the **cell 3**. The irregularity in the left side of the figure can be sight of an irregular wetting or electrode plating, which might lead to a higher initial capacity. The behavior in the right side might mean a phase change of the layered material, by a change of valency of the transition metal (Ni).

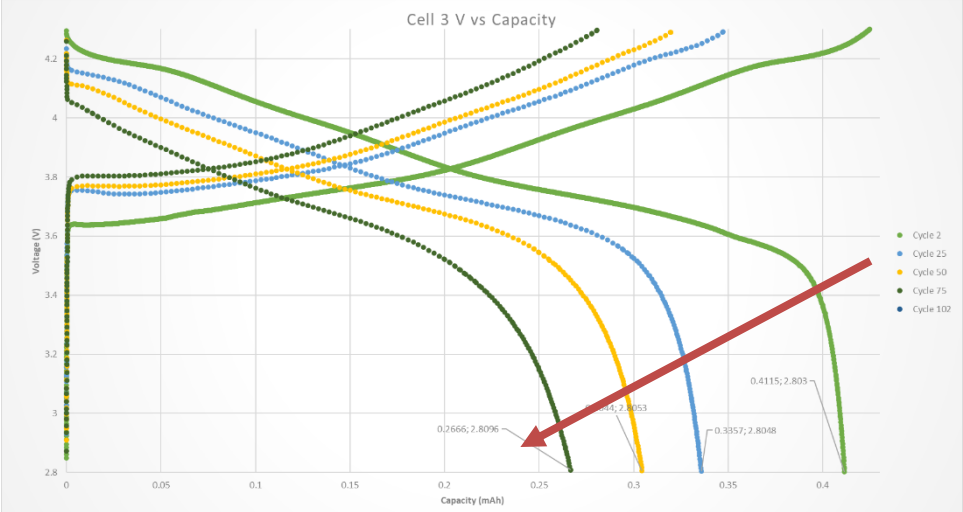

Figure 6.7 - Voltage vs capacity profile cell 3

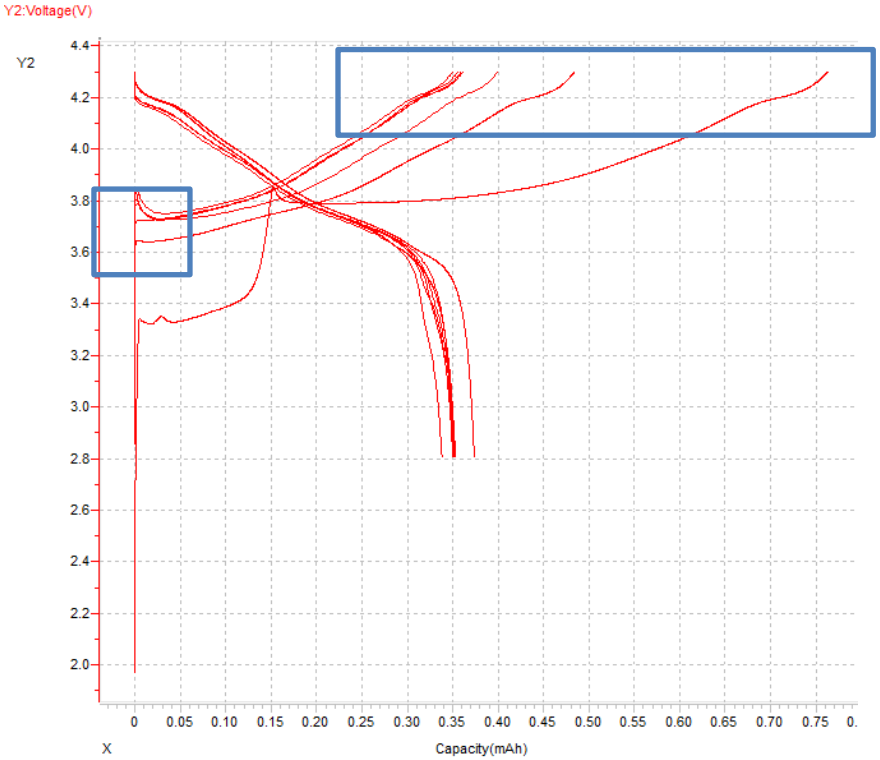

Figure 6.8 - Voltage vs capacity profile, cycles 1-7 cell 3

We can see in detail the voltage profile of the cell 3 considering just the first cycles. It is noticeable a trend very similar to the voltage profile of cell 1 in the last part of the discharge curve.

The **cells 5** and **6** have a very similar behavior as we can already see in the voltage profiles.

In these two cells we can see a voltage profile that is not so uniform as cell 1 and cell 3. The decay is evident as the cell before but seems not uniform and there are much more oscillations.

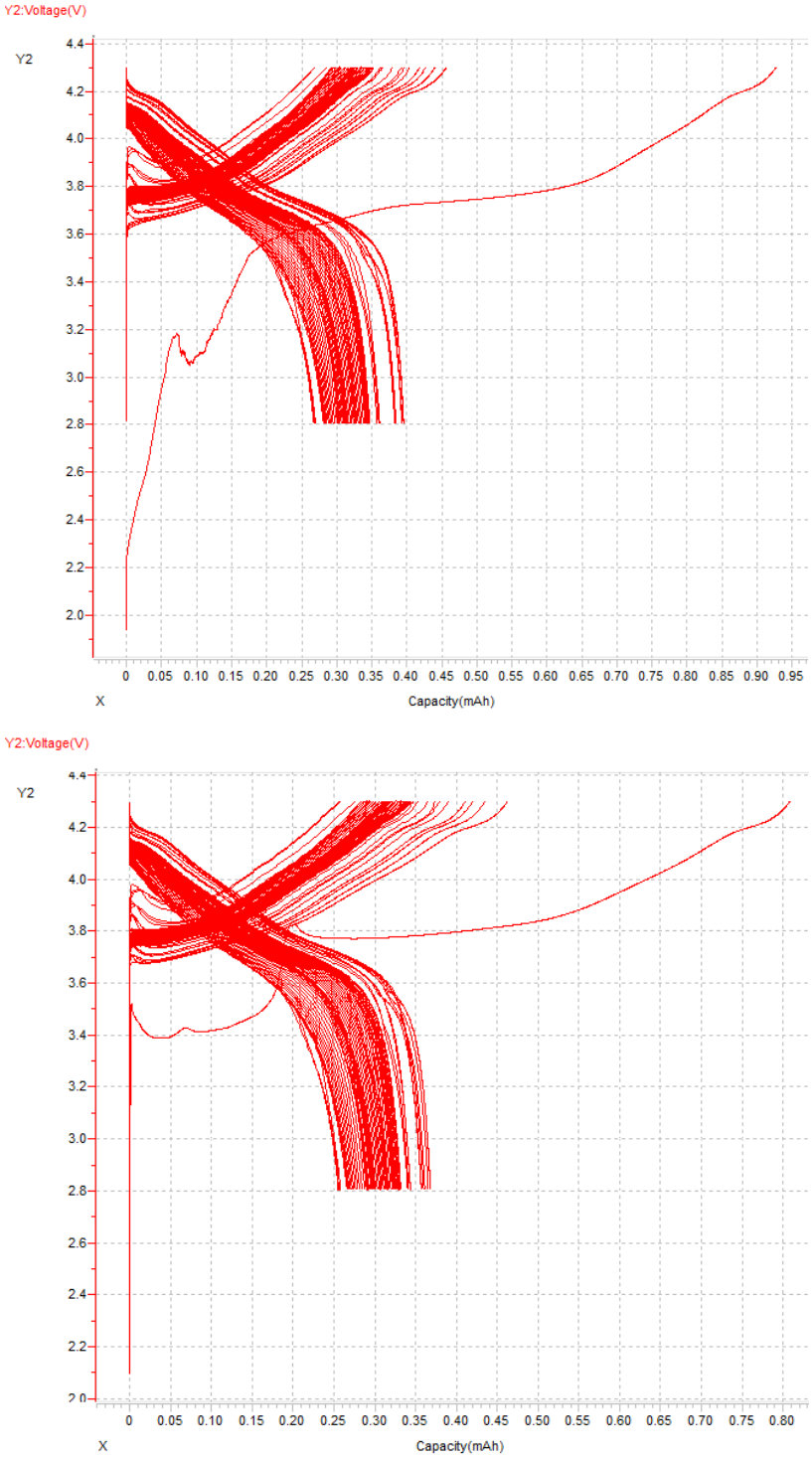

Figure 6.9 - Voltage vs capacity profile cells 5 and 6

Analyzing the voltage profile of cell 5. We have a special behavior at high capacity, the charging curve. One possibility is there's a plateau because the electrode is not connected properly to the electrolyte (less porosity) or to the pure collector (less connective carbon), so we lose capacity. In the first cycle the cell doesn't behave very well because at first there is an oxidation in the electrolyte that should not happen. We could consider the cell anyway neglecting the first cycle.

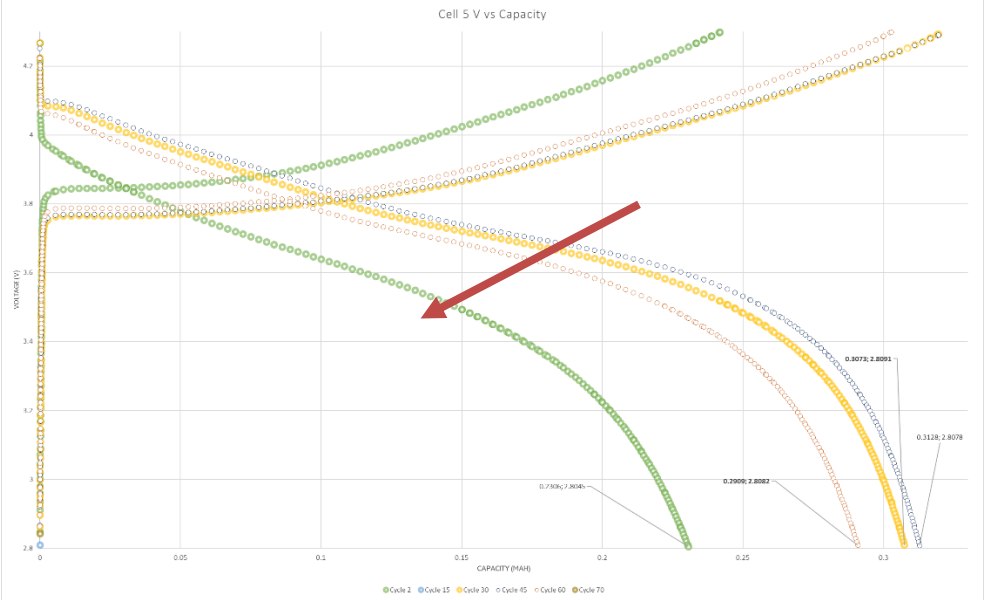

Figure 6.10 - Voltage vs capacity profile cell 5

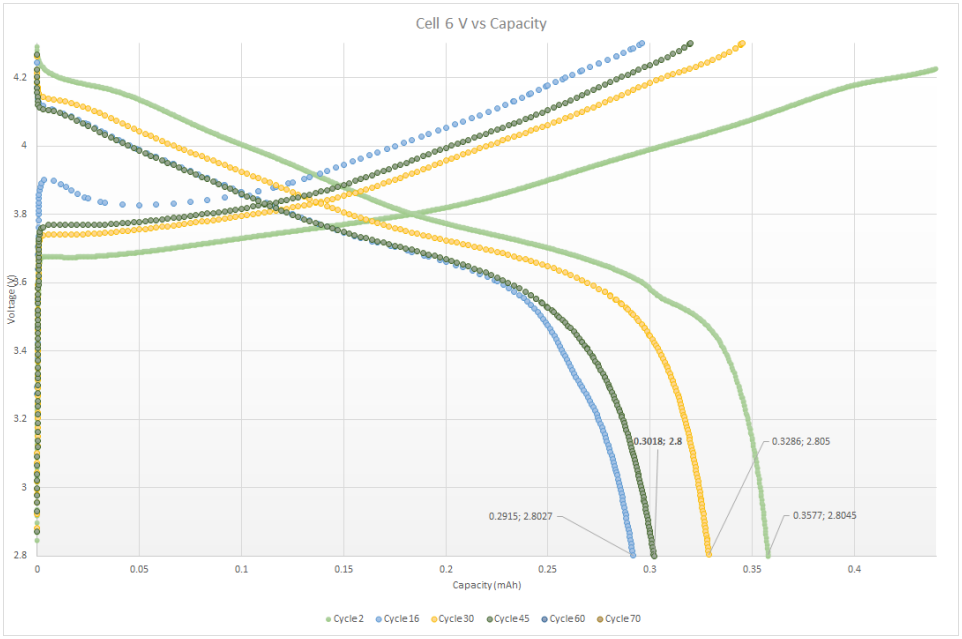

Figure 6.11 - Voltage vs capacity profile cell 6

6.1.3 Charge and Discharge specific capacity

Now we analyse the Charge and Discharge specific capacity varying the cycle ID for all our cells. The charge and discharge specific capacity refers to the amount of charge that can be stored and delivered respectively per unit mass. The specific capacity usually uses mAh/g. The charge specific capacity represents the amount of charge that the battery can store during the charging process. It indicates the maximum capacity of the battery to hold electric charge and usually it is higher than the discharge specific capacity. The discharge specific capacity refers to the amount of charge that a battery can deliver during the discharge process. This value corresponds to the usable capacity of the battery during its discharge cycle. Because of internal resistances and efficiency losses during the discharge this value is lower than the charge specific capacity. The specific capacities vary with the battery chemistry, size, manufacturer, and other factors.

In the first cycle of the **cell 1** we have too high capacity, so it seems to be contaminated like happens LFP. In this cycle we have 145/210= 0.69 efficiency so we lose the 30% and we will keep decrease in the next cycles. The 30% loss can be in part, since Lithium can take up the place of some Ni atoms in the crystal structure of the cathode., which affects the diffusion of Li+ ions through the crystal structure. If this occurs the cathode capacity will deteriorate even if the metallic Li anode supplies an unlimited supply of Li^+, because the diffusion rate of Li+ is hindered, even if new Li is supplied by the Li-Metal anode. There are oscillations because of the night-day (temperature variations) shift but the main trend is good.

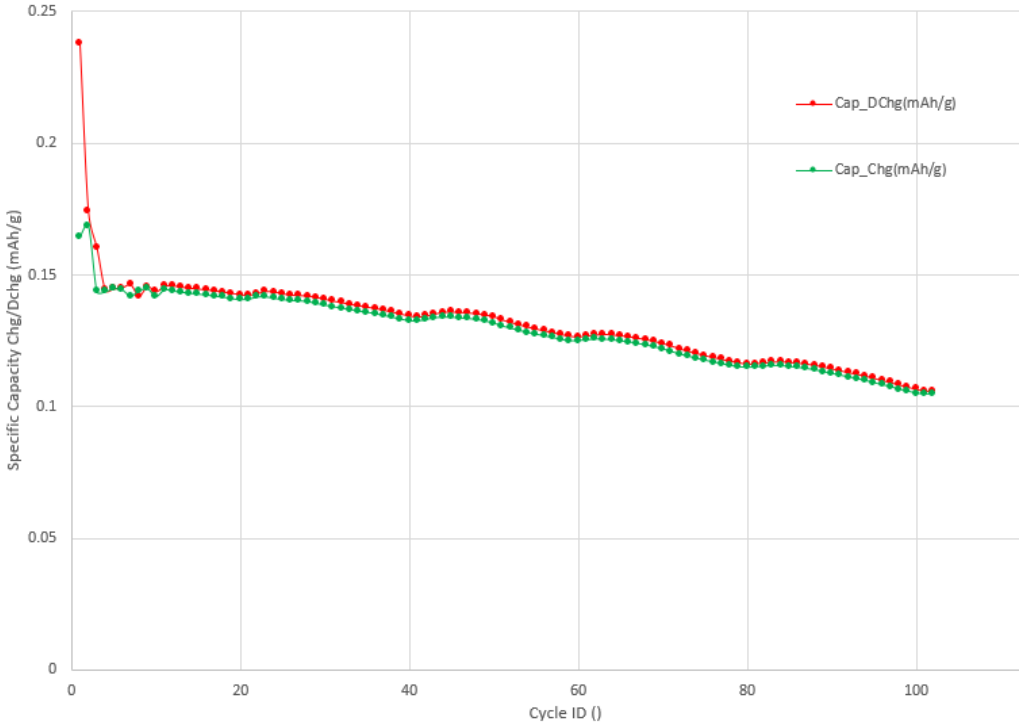

Figure 6.12 – Charge and Discharge specific capacity vc Cycle ID, cell 1

The specific capacity trend of the **cell 3** is the same as Cell 1 but it's evident that in the first cycle we have a lower capacity than cell 1 that is like 46% so we have a 54% loss, so much higher losses.

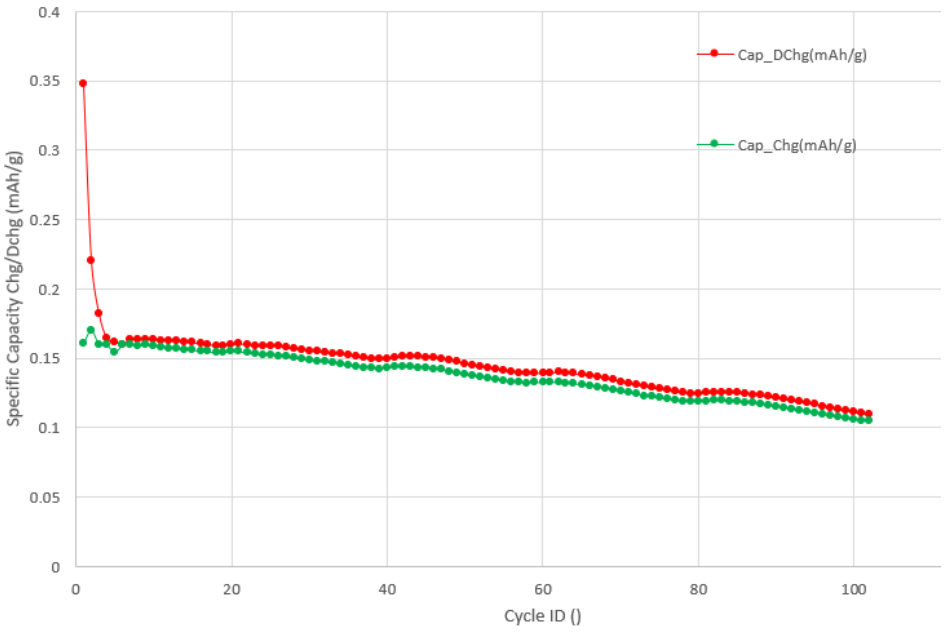

Figure 6.13 - Charge and Discharge specific capacity vc Cycle ID, cell 3

In the first cycles we can see a capacity decay but then after few cycles it recovers. This means we didn't destroy the system with the C-rate. The Charge and Discharge specific capacity trend of **cell 5** and **6** is very similar.

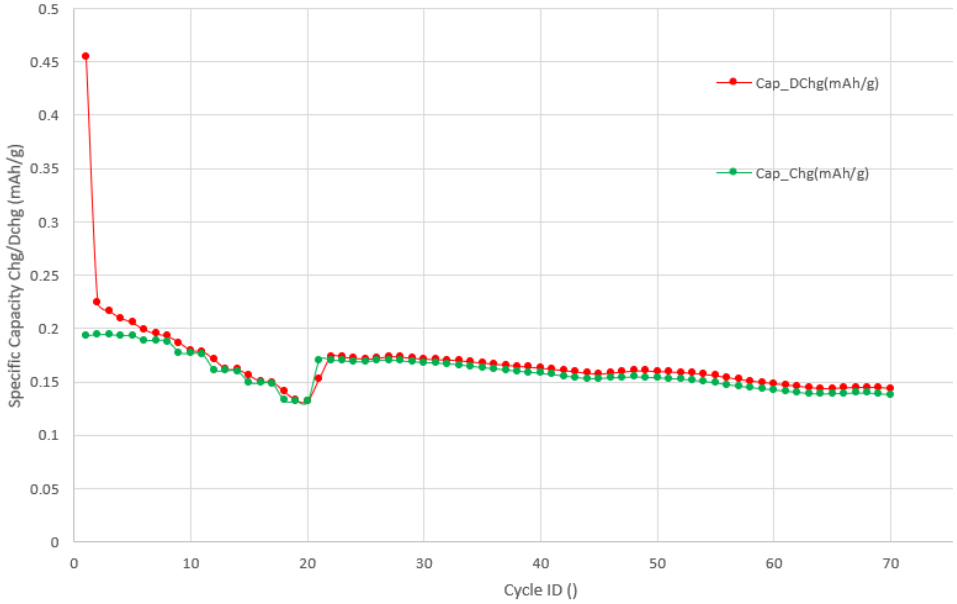

Figure 6.14 - Charge and Discharge specific capacity vc Cycle ID, cell 5

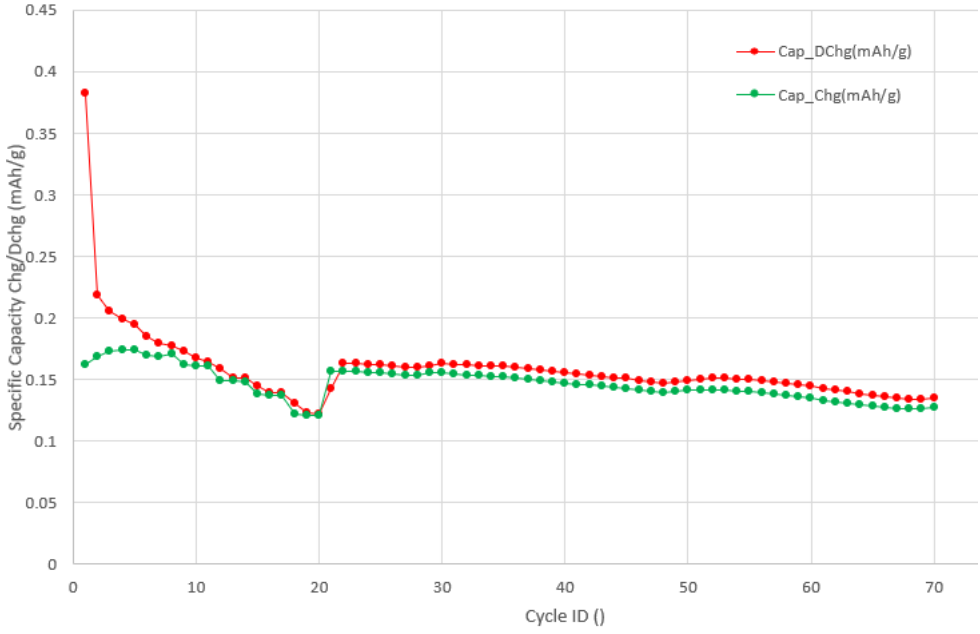

Figure 6.15 - Charge and Discharge specific capacity vc Cycle ID, cell 6

6.1.4 Coulombic efficiency

We analyze the coulombic efficiency of our cells varying the cycle ID. The coulombic efficiency, also called faradaic efficiency or current efficiency, describes the charge efficiency by which electrons are transferred in the battery. It is the ratio between the total charge extracted from the battery to the total charge put into the battery over a full cycle. Li-ion battery has the highest coulombic efficiency which can exceed 99% when it is charged/discharged at a moderate current and at cool temperatures. This efficiency improves with cycling and the Li-ion battery are a very stable battery system. The efficiency reaches values over 100% because the current decreases to 1C. This happens because in the previous cycles at high rates the cathode is not fully delithiated(i.e. charged), which means that charge is limiting and not discharge. As a result of this, the cell was left charged after the C-rate test and can deliver more capacity that is charged in the first cycle. This phenomenon is common for cathodes since the insertion of Li+ is usually more limiting than de-insertion as one induces an increase of concentration and the other the decrease.

The oscillations of the efficiency in the cycle after the first ones are due to the variation of temperature during the night-day shift. The efficiency of the cells should be around 99.9%. However, the efficiency of **cell 1** results around 98.5%. This might be due to contaminating agents in the electrolyte.

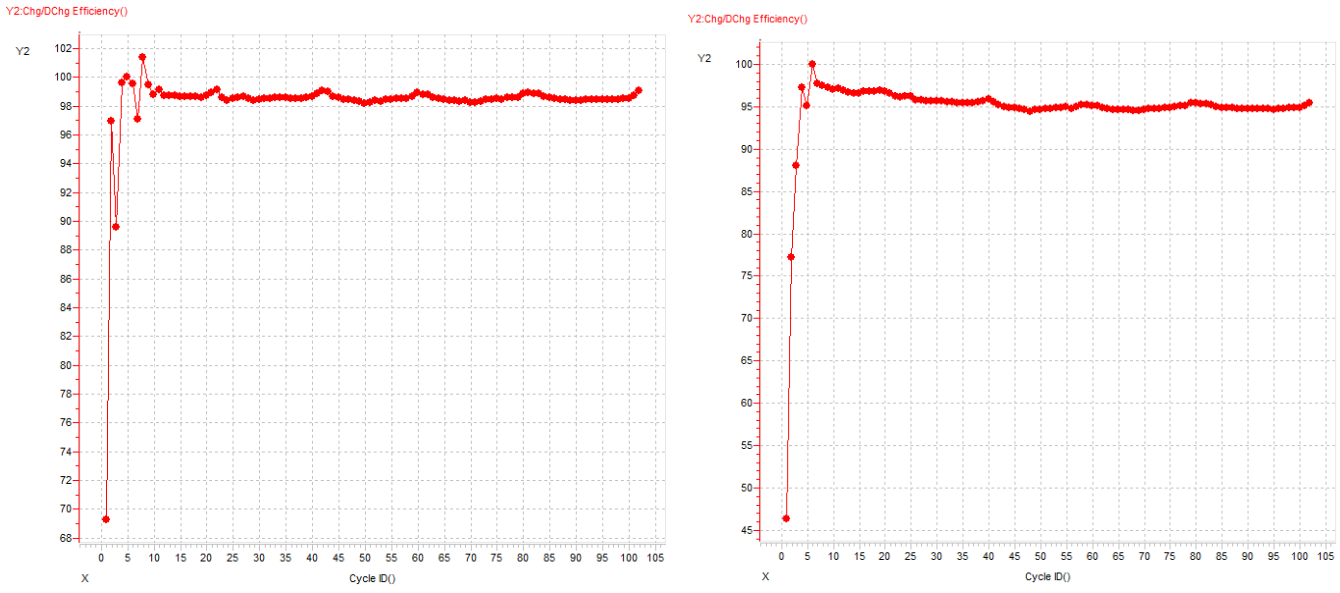

(a) (b)

Figure 6.16 – Coulombic efficiency, cell 1(a) and cell 3(b)

It’s evident that the first cycles of the **cell 3** have a very low efficiency if we compare it with the value of cell 1. However, its trend is more stable than the cell 1 because we have just one oscillation. In the later cycles we have an efficiency that goes from 94% and 96%. It’s very low for a NMC battery for this reason it doesn´t perform well.

The efficiency trends of the **cell 5** and **6** are almost identical as we can see from figures 6.17 and 6.18, respectively. The first cycle are both at 42% but the cycles from 2 to 7 of the cell 6 are at lower efficiency but the two cells reach at cycle 8 an efficiency higher than 95% and from this point they behave almost the same. Comparing the values with cell 3 we have higher efficiency but still lower than the cell 1. The cell 1 seems to perform the best. So, these two cells are good after a few cycles for their performance otherwise they don’t reach the topical efficiency higher than 98% as cell 1.

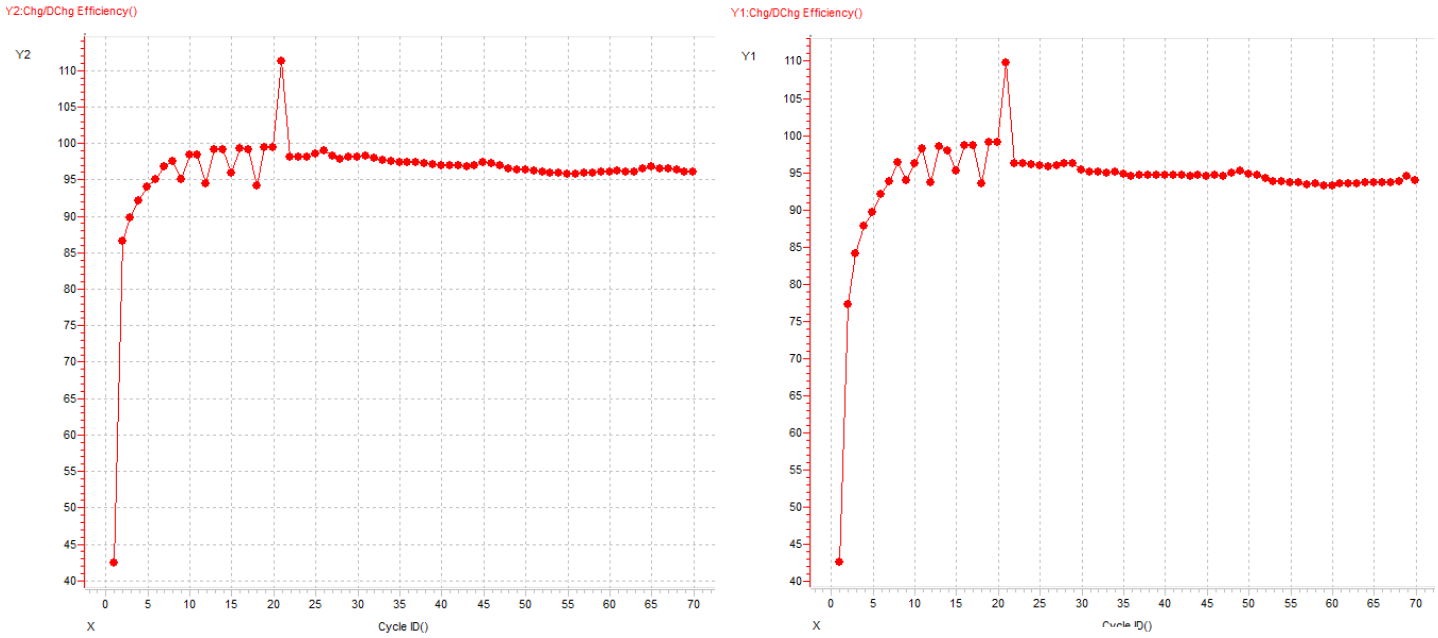

(a) (b)

Figure 6.17 - Coulombic efficiency, cells 5(a) and 6(b)

6.1.5 Specific capacity discharge

It represents the maximum amount of specific energy that the battery can deliver per gram of active material. In our case cathode of the battery is the active material (80% wt NMC-811). The unit of Specific Capacity Discharge is mAh/g.

This chart depicts the Specific Capacity discharge of **cell 1**. We can see in the first cycles we used low current, so the specific capacity is higher. It is evident a huge drop from cycle-2 to cycle-3 because the C-rate changes. So, the capacity at 1C is lower the capacity at 0.1C as we expected. From cycle-3 there is a steady decline in this cell. At the end of the test the cell has the specific discharge capacity at 94.75 mAh/g (cycle ID 102, figure 6.19).

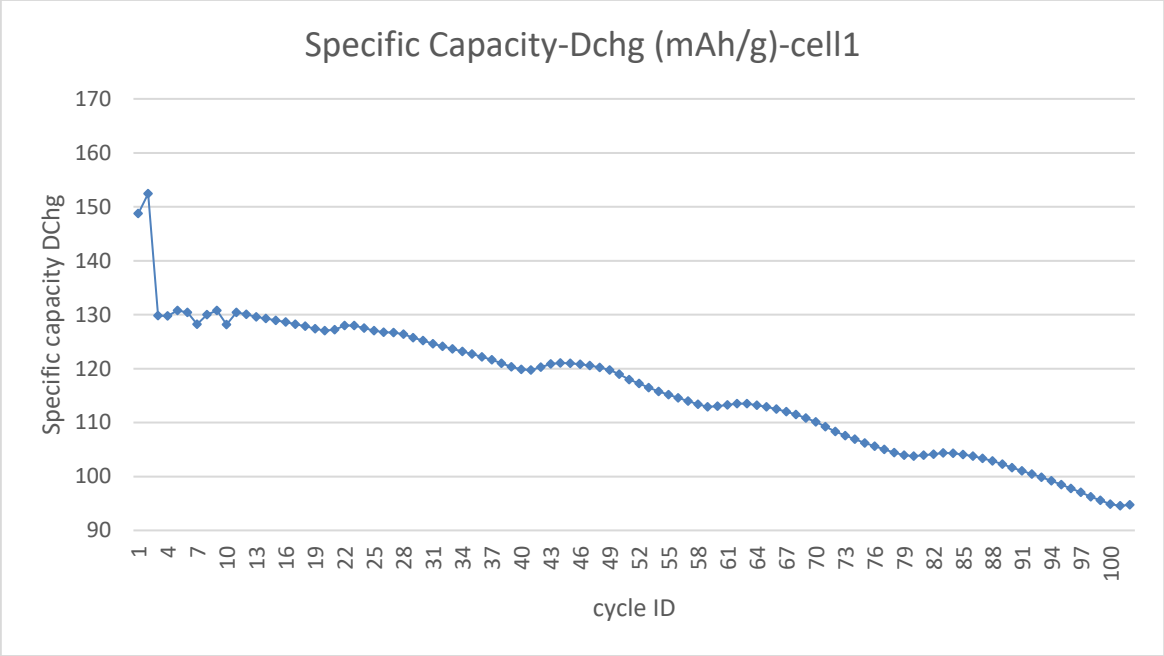

Figure 6.18 – Specific capacity discharge vs cycle ID, cell 1

In the **cell 3** there is a noticeable fall in the 5th cycle. From cycle-6 there is a steady decline until the end of the measuring campaign. Compared to the other two cells, cell 3 is much steady in Specific Capacity discharge.

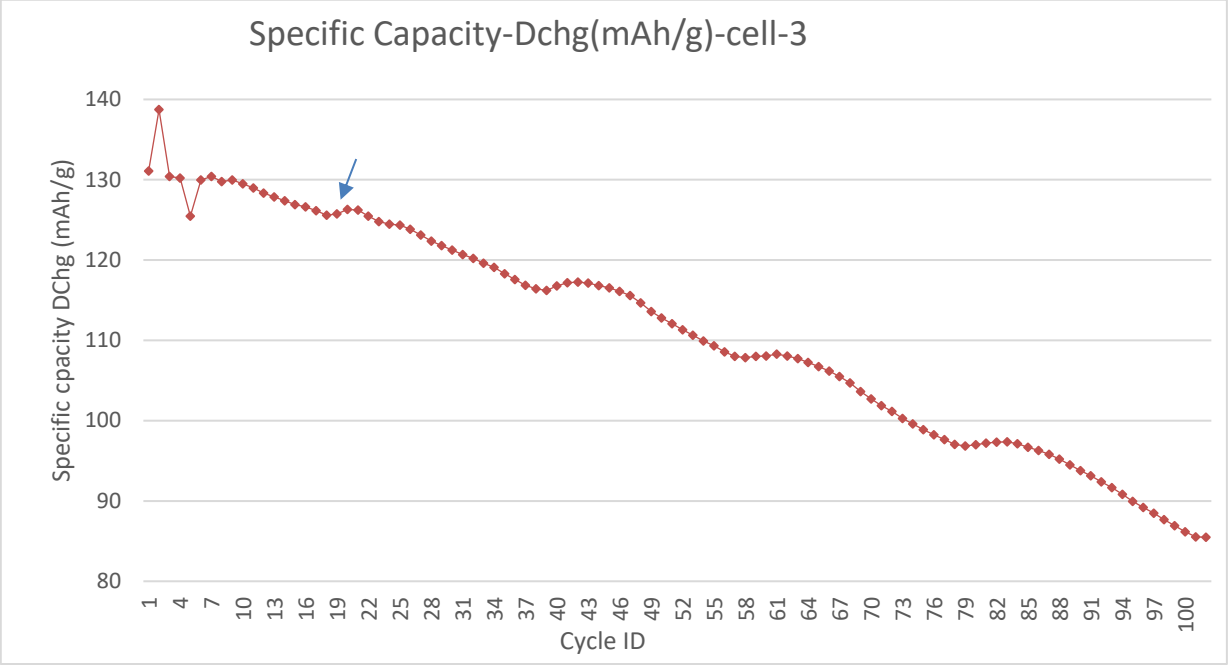

Figure 6.19 - Specific capacity discharge vs cycle ID, cell 3

Cell 6 has rose slightly till cycle 6 and has a gradual fall till cycle 20 due to the increase of C-rate. Then there is a slight increase at the 21st cycle from 89 to 114 mAh/g (marked with a blue arrow in figure 6.21) due to the decrease of C-rate.

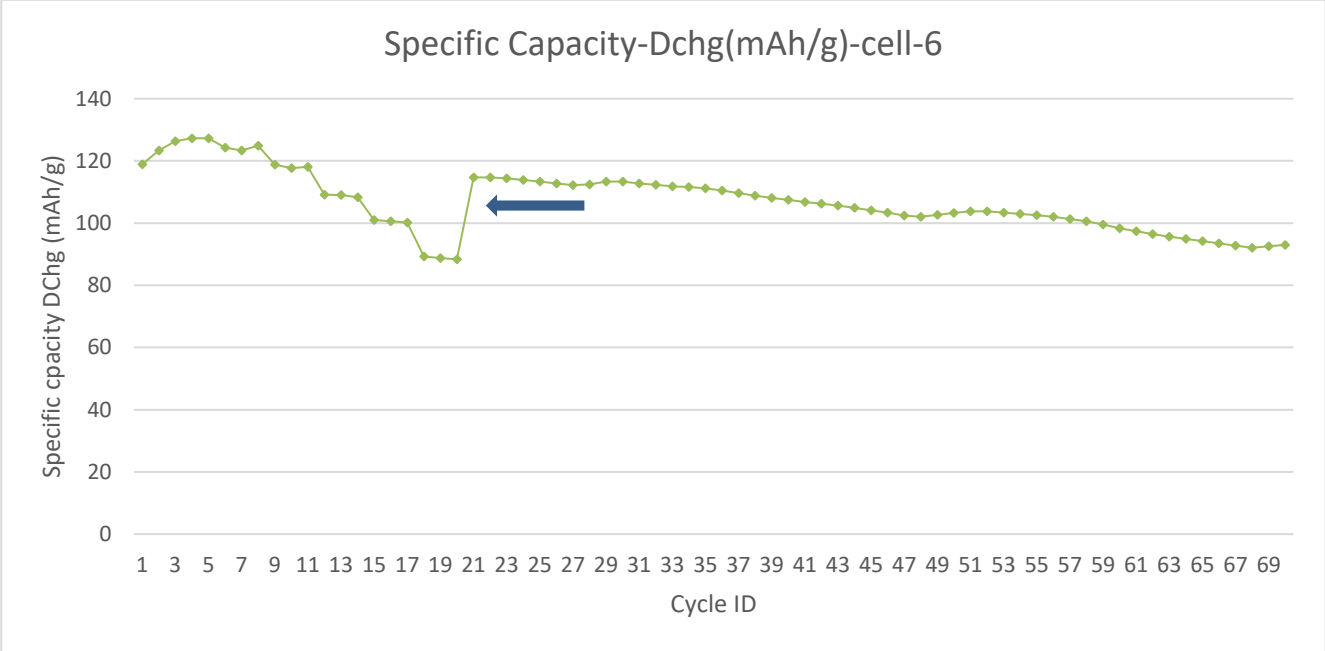

Figure 6.20 - Specific capacity discharge vs cycle ID, cell 5

Finally, we can compare the specific capacity of all our cells in the graph exposed in *figure 6.22.*

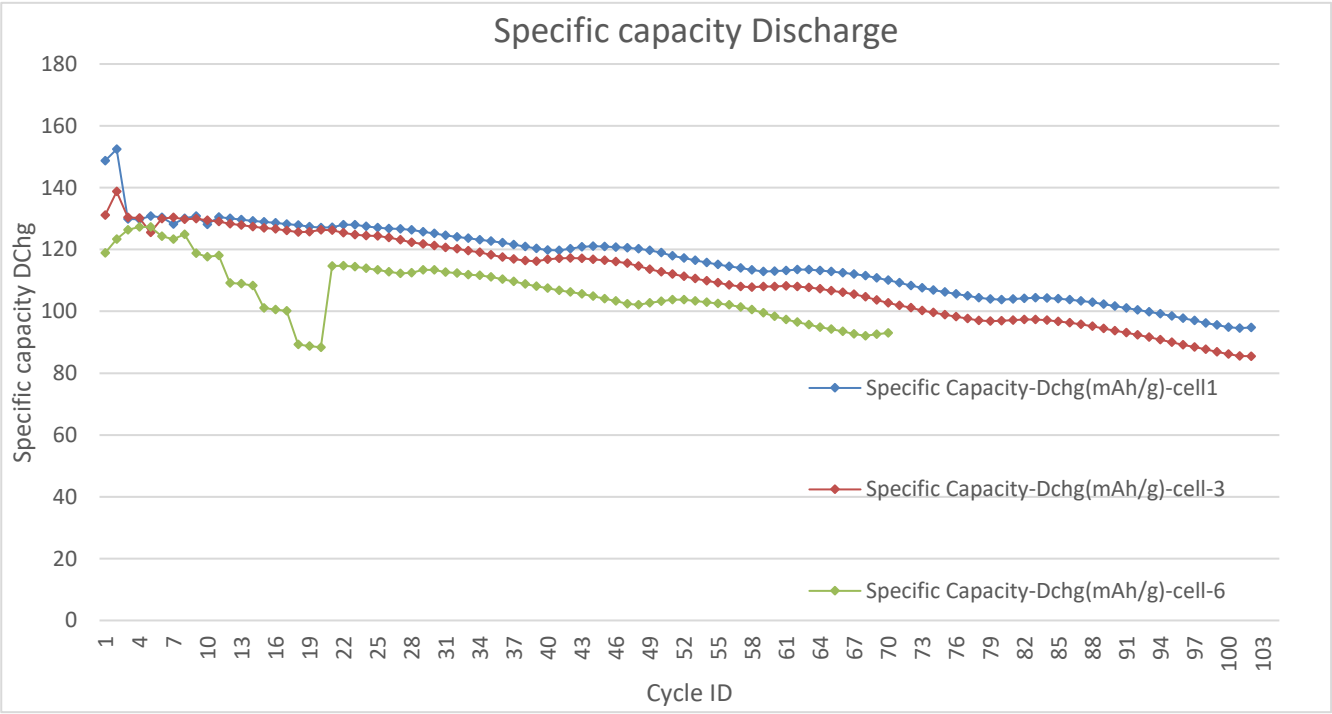

Figure 6.21 - Specific capacity discharge vs cycle ID

6.1.6 Capacity fading analysis

The first part of our cycling it is done at varying Crate as it is evident in the figure then after the cycle 23 we work at constant Crate=1. The procedure have been repeated for all the cells in analysis. As

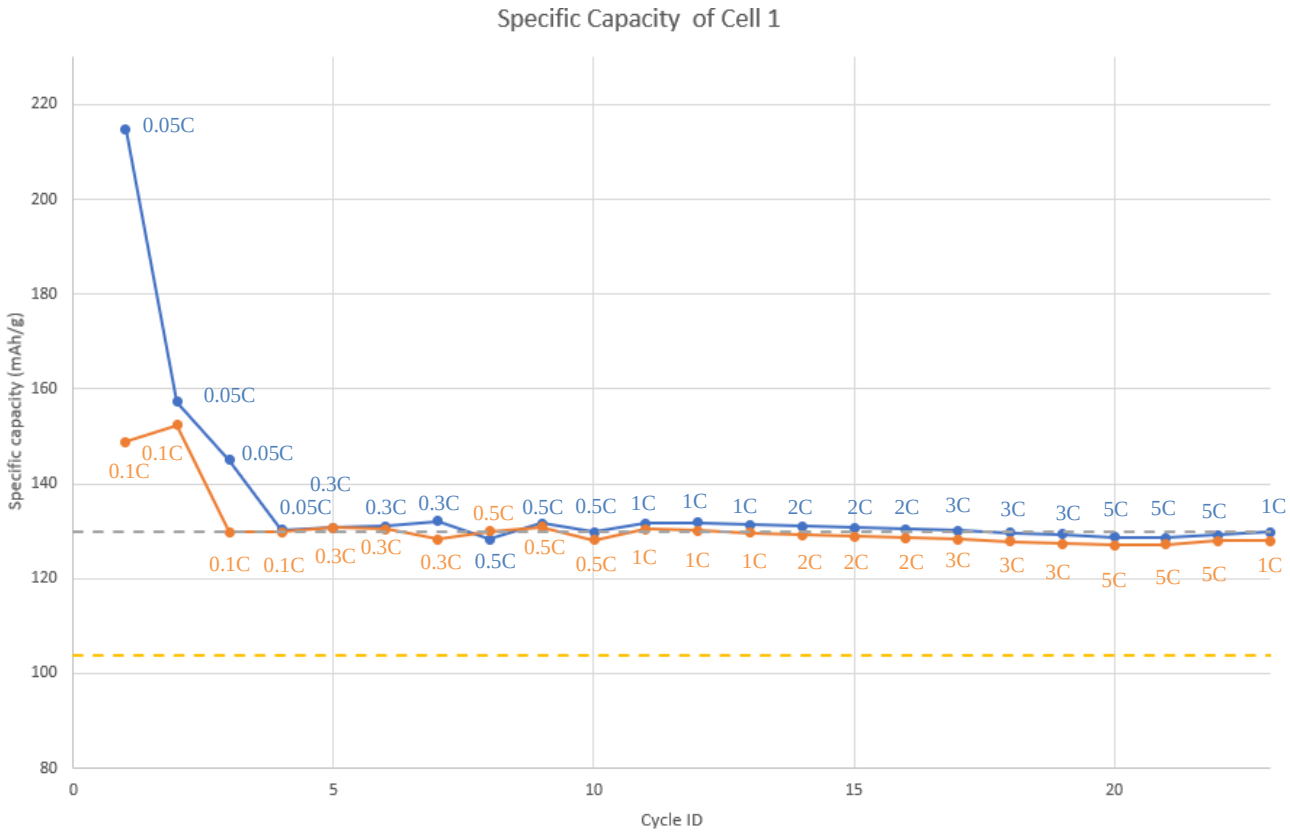

Figure 6.17 – Specific capacity vs cycle ID, cell 1 at different C-rates

we can see from the graph the specific capacity charging has a steep decrease from the cycle 1(214,82 mAh/g) to the cycle 2(157,31 mAh/g) then the difference from the specific capacity charge and discharge decreases because the efficiency increases. It's evident a slight decrease from the Crate=1 to Crate=5 due to the increase of the Crate.

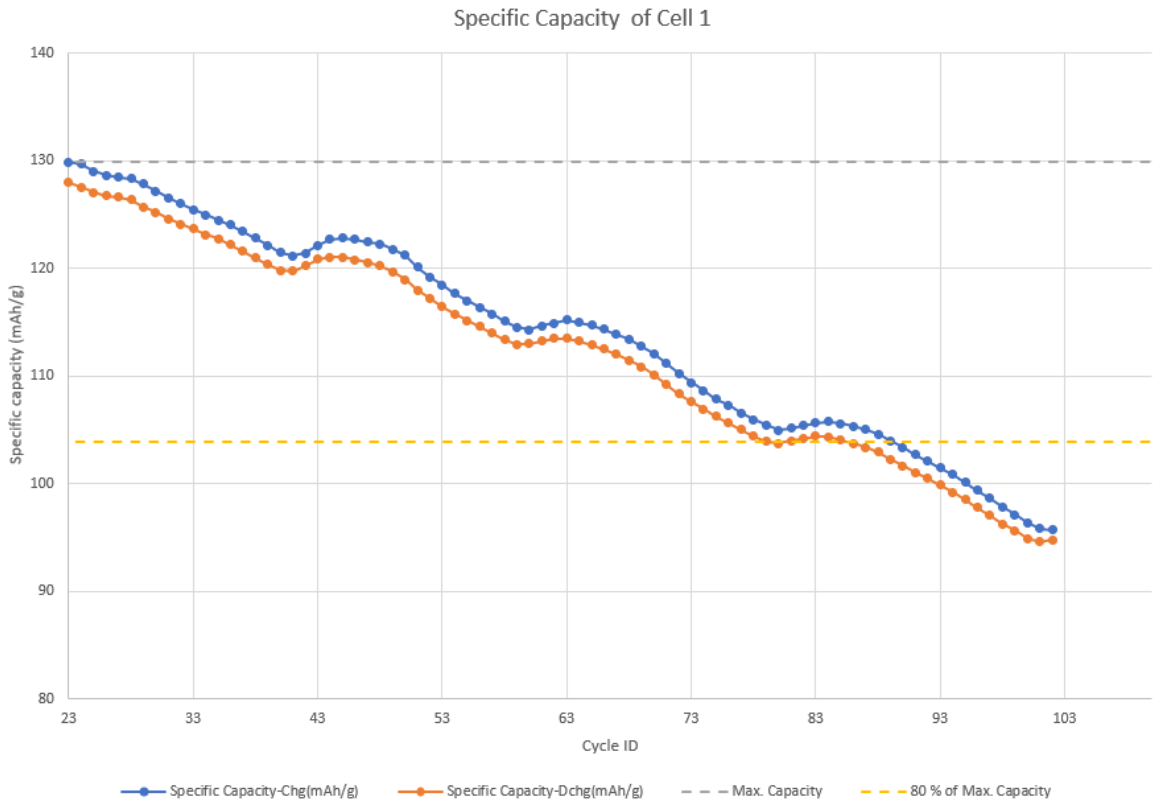

Figure 6.18 – Specific capacity vs cycle ID, cell 1 Crate=1

We analyzed the number of cycles needed before reaching the 80% of the maximum specific capacity at a constant C-rate = 1 in the figure. Oscillations probably due to temperature variations (not controlled variable). In **cell 1** we reach 80% of the max. specific capacity at cycle 90 so it's good performance.

The cell 3 as the cell 1 has a steep decrease of specific capacity charging from cycle 1(283,12 mAh/g) to cycle 2(179,68 mAh/g). The behavior varying the Crate is more steep than the cell 1 because for example from the cycle 19(3C) TO 20(5C) in cell 1 the difference between the specific capacity charging is 0,5094 mAh/g and for the cell 3 is 0,6088 mAh/g.

It's evident that the **cell 3** has a faster capacity fading because reaches the 80% before, 55 cycles (compared to the 68 cycles for cell 1). The **cell 5** and **6** have an identical behavior and reach the 80% of maximum specific capacity after 51 cycles so it seems that these two cells have a better performance.

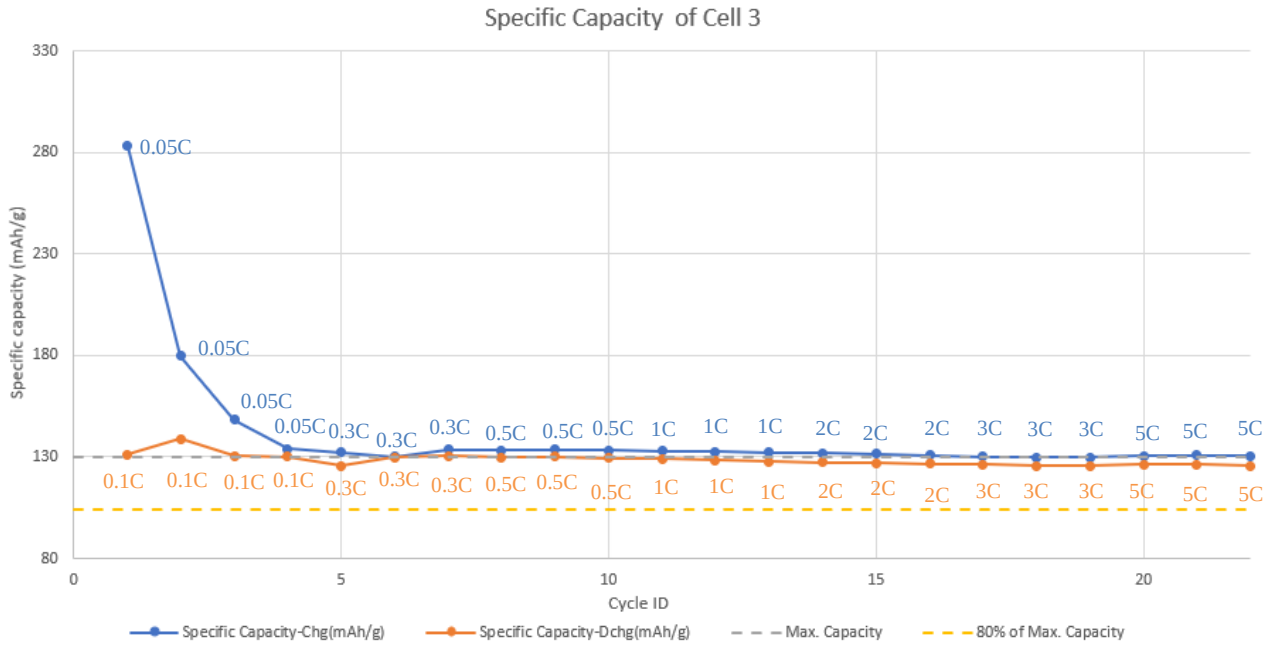

Figure 6.19 – Specific capacity vs cycle ID, cell 3 at different C-rates

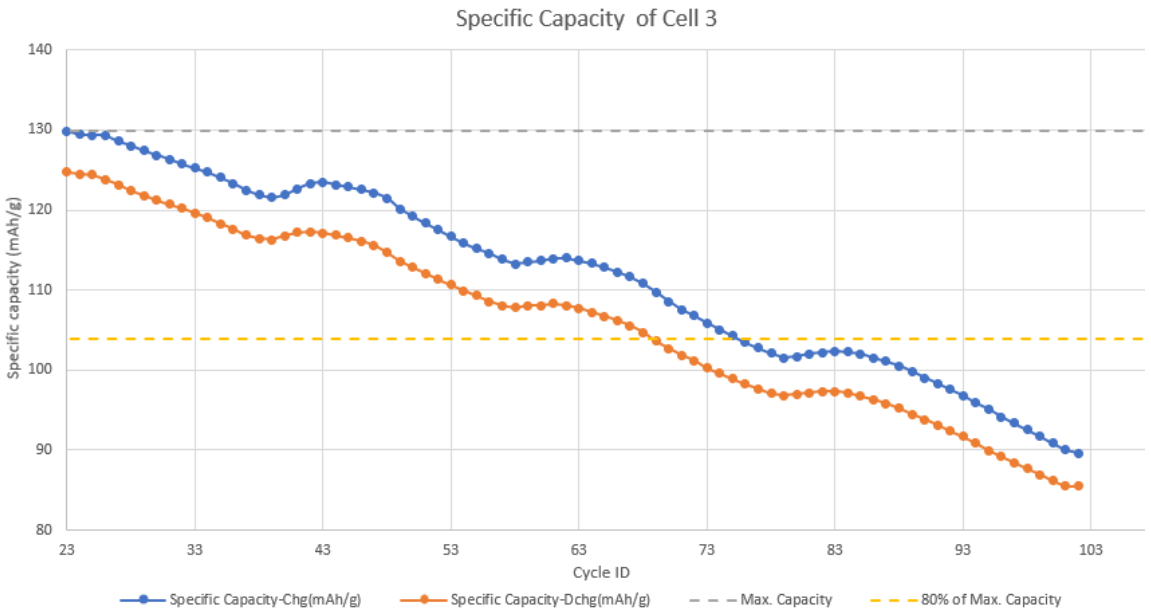

Figure 6.20 – Specific capacity vs Cycle ID, cell 3

The cell 5 and cell 6 have the same behavior. These two cell have a steeper variation of the specific capacity in fact the charging specific capacity vary from the cycle 1(279,29 mAh/g) to cycle

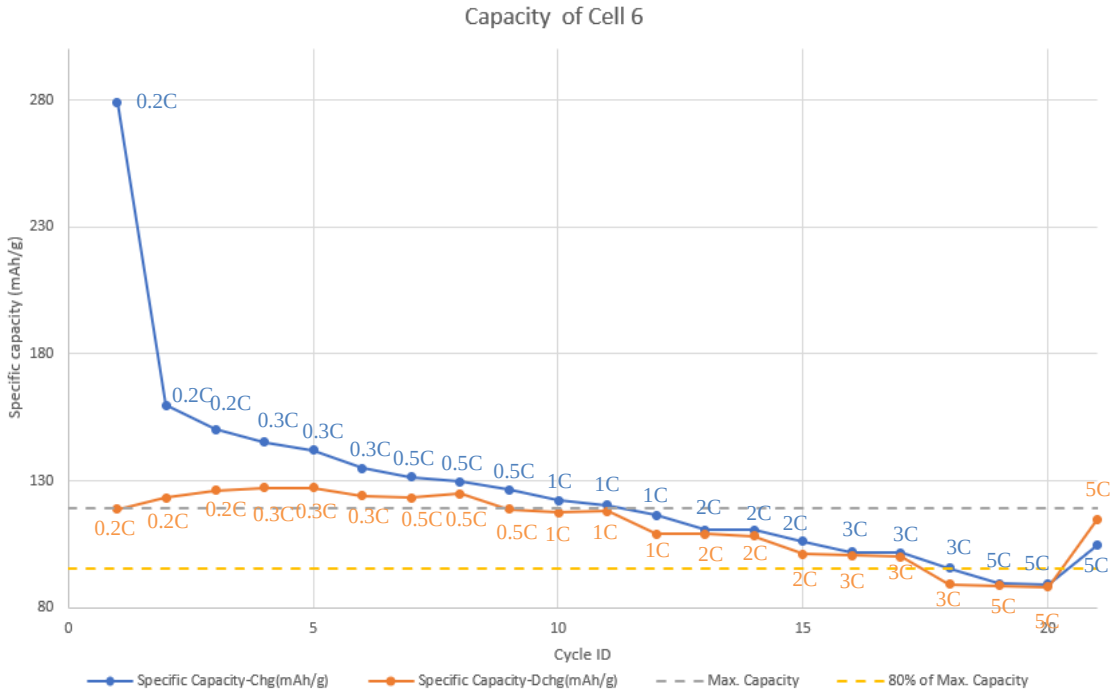

2(159,93 mAh/g). The distance from the values of specific discharging and charging are vary high at the first cycles and then decreases when increases the efficiency. It is evident a sharper decrease

of charging specific capacity changing the Crate, in particular around cycle 18. From cycle 17 we go from a value of 101,63 mAh/g to a value of 95,56 mAh/g for the specific capacity charging.

Figure 6.21 – Specific capacity vs cycle ID, cell 6 at different C-rates

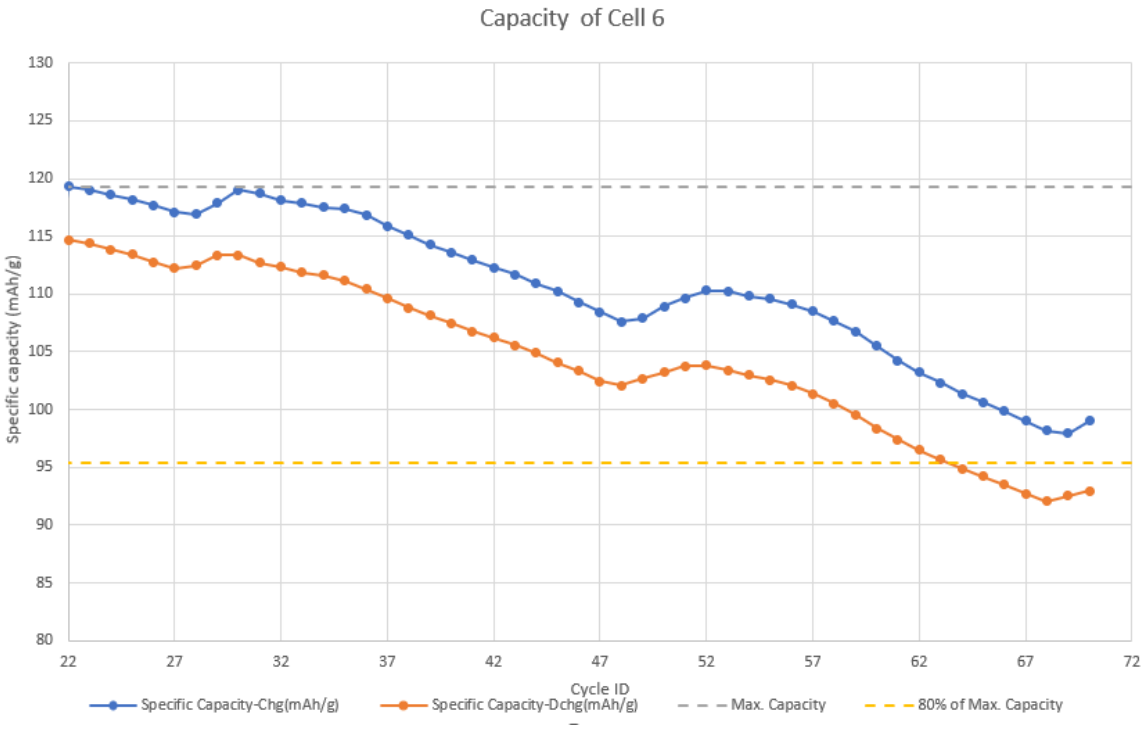

Figure 6.25 – Specific capacity vs Cycle ID, cell 6

The change of the C-rate it's evident also in the figure 6.25 and the cycles correspond to the specific capacity graph, figure 6.15.

The capacity fading results are in table 6.3.

Cell Number	Charge			Discharge		
	Start	End	n cycles	Start	End	n cycles
1	23	90	68	23	89	67
3	23	77	55	23	75	53
5	22	72	51	22	72	51
6	22	72	51	22	72	51

Table 6.3 – Capacity fading results

6.2 Full Cell testing

After characterization of the cathode material in the half cell tests, we assembled full cells to evaluate the overall battery performance. The full cells consisted of an NMC811 cathode, either Graphite or SiC as the anode, a separator, and an electrolyte.

The full cell testing primarily involved charge-discharge cycling and capacity retention measurements. Charge-discharge cycling was performed by applying a predetermined current or voltage profile to the full cell and monitoring the resulting charge and discharge capacities. This test allowed us to assess the energy storage capabilities, efficiency, and cycle stability of the coin cell battery system.

Additionally, capacity retention measurements were conducted to determine the long-term stability of the full cells. These measurements involved periodically charging and discharging the coin cells and calculating the ratio of the discharge capacity to the initial capacity. A higher capacity retention indicated a more stable battery system with reduced capacity fade over time.

The data obtained from the full cell testing allowed us to evaluate the overall performance of the coin cell battery system, including its energy storage capacity, power output, cycle life, and stability.

6.2.1 Voltage vs capacity profile

Initially, we can see the fact that the first charging process carried many irreversible reactions which consumed and locked lithium, probably within the interstitial spaces in the case of the NMC cathode as was explained in the half cell analysis, formation of the SEI in both electrodes.

This might explain the fact that the first cycle of pristine material, carries an important capacity loss (see *figure 6.27*, comparing the two blue arrows, signaling the difference in capacity between charging process of cycle 1 and charging process of cycle 2).

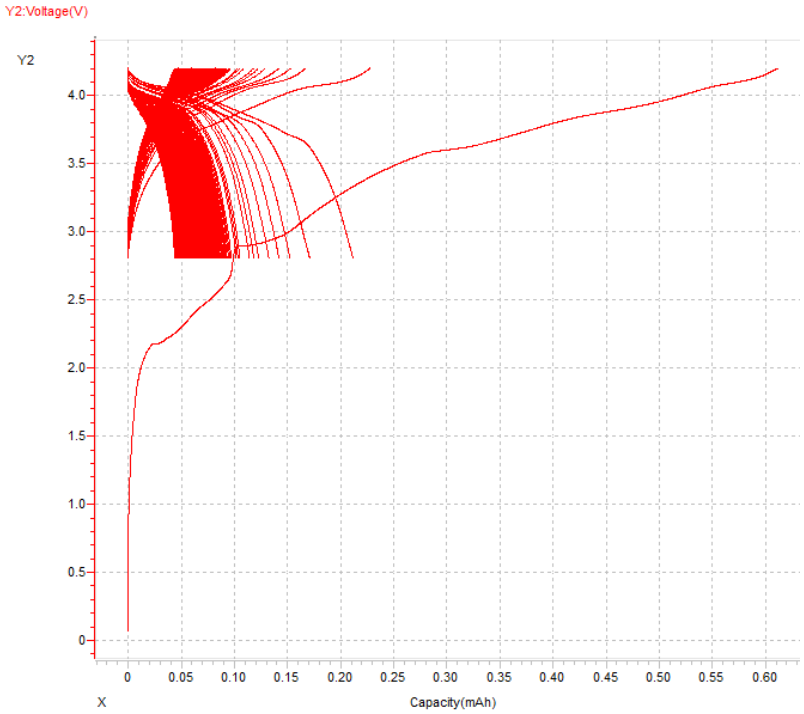

Figure 6.26 – Capacity vs Voltage profile, cell 1

This figure, it's more evident that the material carried more than one phase change during the polarization process. For layered materials (as in the current case with NMC811) is a tougher challenge to identify phase changes when compared to 1D (LiFePO4) or 3D (LiMnO2) cathodes, who both present major characteristic phase changes during normal battery charge/discharge.

The fact that the testing is taking process via a two-electrode system makes it difficult to determine which contributions are from the anode and which are from the cathode (in comparison to a three-electrode system where both anode and cathode are compared to a third Li-metal electrode).

This phase change might be a contributor to the capacity fade of the cell, because when operating with intercalating cathode electrodes such as is the case of NMC (811) (cell 1 case), the reversible storage of Li+ doesn't require phase changes to be made in such a way that in the voltage range, an extended plateau is visible.

For this reason, the phase changes occurring are in general undesirable, except for the graphite anode where graphite carries 4 main phase changes during Li+ intercalation (charging), which corresponds to a normal operation (5).

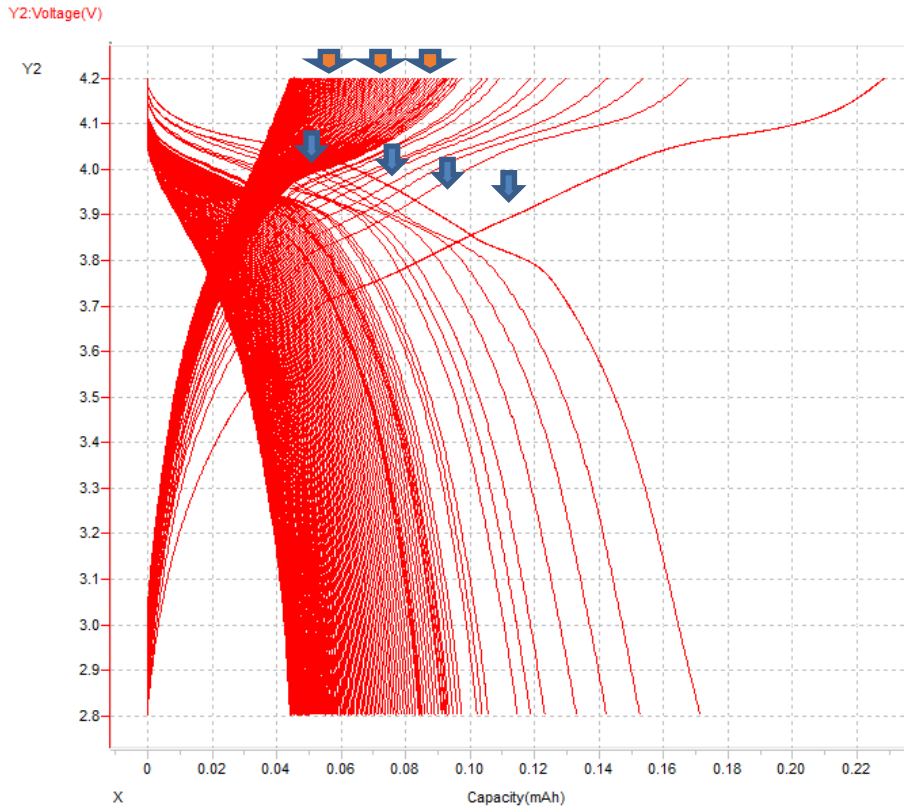

Figure 6.227 - Capacity vs Voltage profile, cell 1 without cycle 1

Some of the phase changes presented in one of the electrodes are exposed with a blue arrow in *figure 6.29. It´s* evident that there´s a recurring phase change during the discharge process which keeps

being present every time at a higher voltage (see blue arrows that appear higher in the vertical axis, presenting a similar plateau, and assigned to the same phase change occurrence).

The voltage at which the phase change occurs is in theory happening at a given constant voltage. However, the fact that here it´s gradually rising as the number of cycles increase, can be related to the fact that the test bench has the objective of keeping the cell voltage within the same range, even though the degradation of the electrodes leads to a gradual decrease in the cathode´s potential. This is countered by an increase in the cathode´s potential, reducing the net voltage difference.

This can be a reason for accelerated degradation because the lithium (de-)intercalation in the anode is forced, hence leading to microcracking of the SEI due to a more energetic pass of cations through this layer due to the increased voltage, leading to deformation and subsequent reconstruction of the SEI. This leads to a depletion of lithium stocks of the full cell.

This could be part of the explanation for the ever-increasing degradation that led to a capacity loss, pointed with the blue arrow (in *figure 6.33*).

Another argument in favor of the possible repetitive unreversible reaction occurrence during each cycle, is the fact that the initial plateau presented during charging gradually disappears, and after several cycles, the behavior changes from an initial plateau (see *figure 6.31*, orange arrow), towards a different slope that keeps rising without the presence of the previous evident plateau (see *figure 6.31*, blue arrow).

This could represent the fact that this initial plateau forms part of some semi reversible reaction, that initially was able to be partially returned to its original form, but after several cycles was no longer able to be reversed, leading to an amount of active material to be lost during the cycling process.

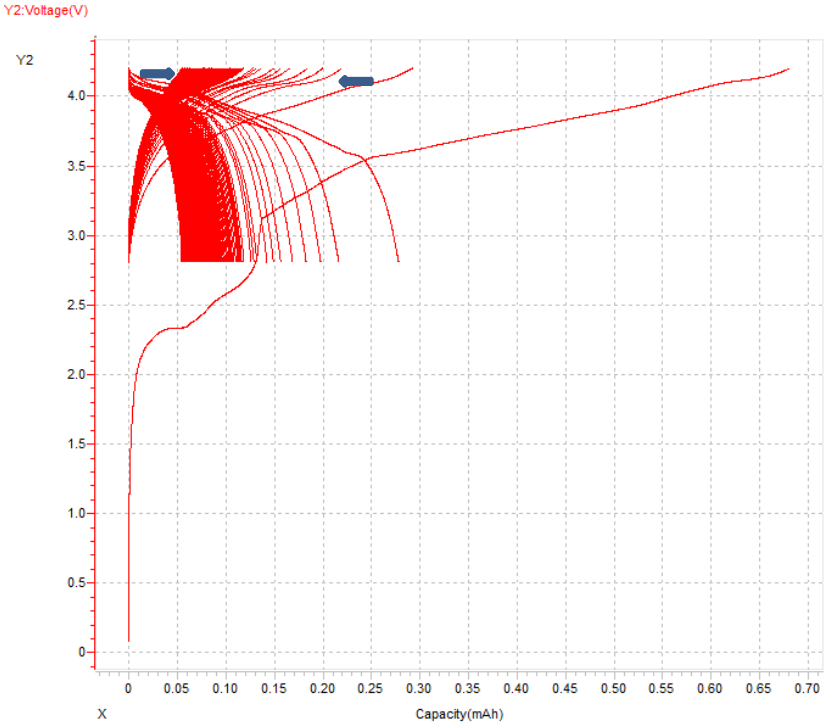

Figure 6.2823 - Capacity vs Voltage profile, cell 2

During the first charge, the initial voltage is almost zero, as the full cell assembly is done with the cell discharged in the charged state.

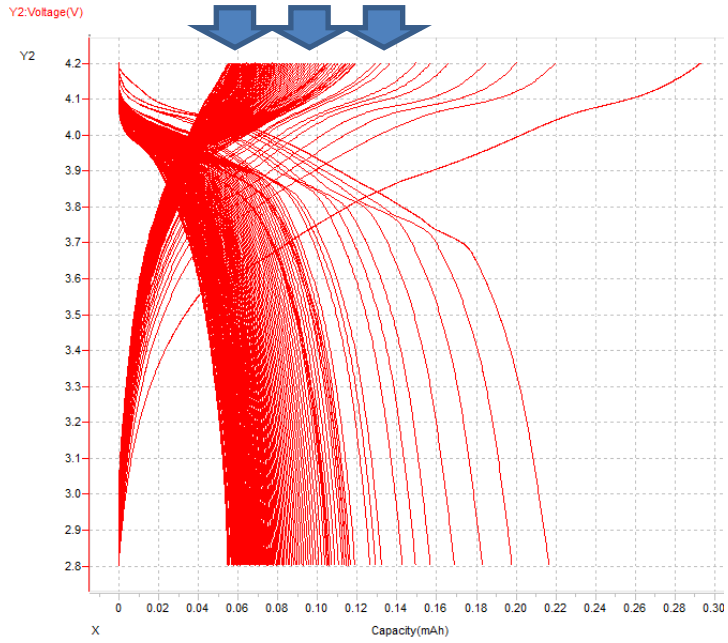

Figure 6.2924 - Capacity vs Voltage profile, cell 2 without cycle 1

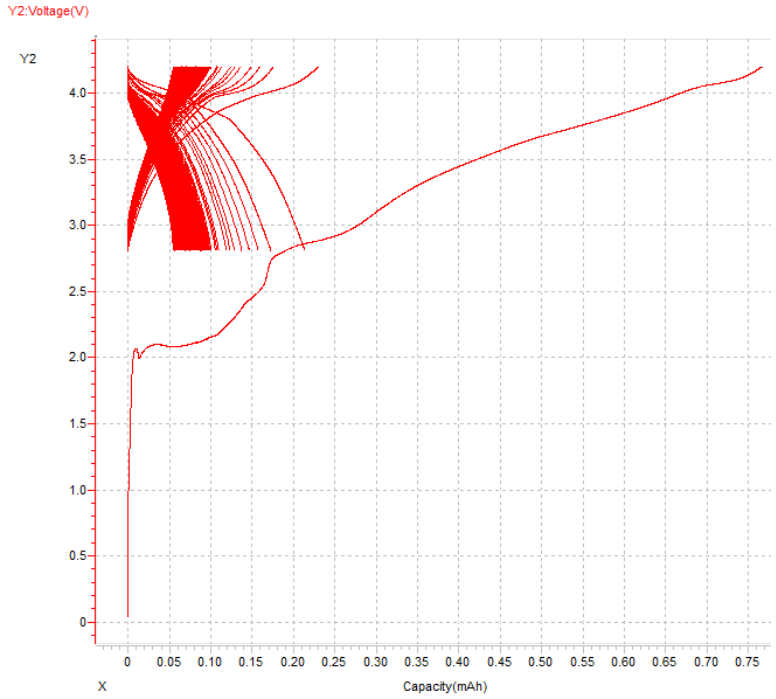

Figure 6.30 - Capacity vs Voltage profile, cell 3

The hypothesis of an increase in voltage with the aim of countering the degradation of the cell loss of active material could be an explanation for the graphite anode performance in cells 1 and 2, and also could explain the current performance of the full cell utilizing Si anodes, as is the case for cells 3 and 4 because this material also hosts Li+ ions intercalated between planar atomic dispositions, as graphite does, however, its spacing is much smaller in comparison to the graphite interlayer spacing (0.233 nm vs 0.334 nm (6)). Hence, experiences a higher tortuosity with the intercalation and deintercalation of ions in this space because the material must stretch more to execute the same action of storing the Li cations.

The previous statement is evident when comparing *figure 6.35* and *6.36*, which correspond to the Si anode, versus the *6.33* and *6.29*, which correspond to the graphite anode, where both the degradation of the Si is faster (drop of capacity), plus the appearance of the ever-increasing slope at the end of the charging process occurs sooner, which if indeed being the case of the occurrence of a gradual irreversible phase change, would support the proposed previous modes of capacity fade exposed before.

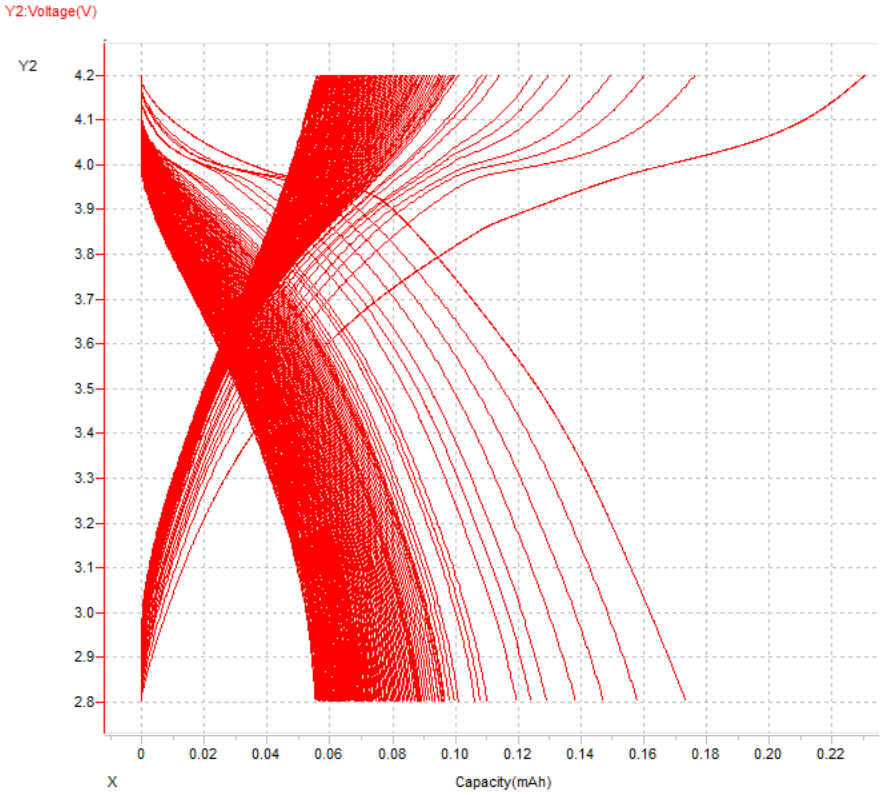

Figure 6.251 - Capacity vs Voltage profile, cell 3 without cycle

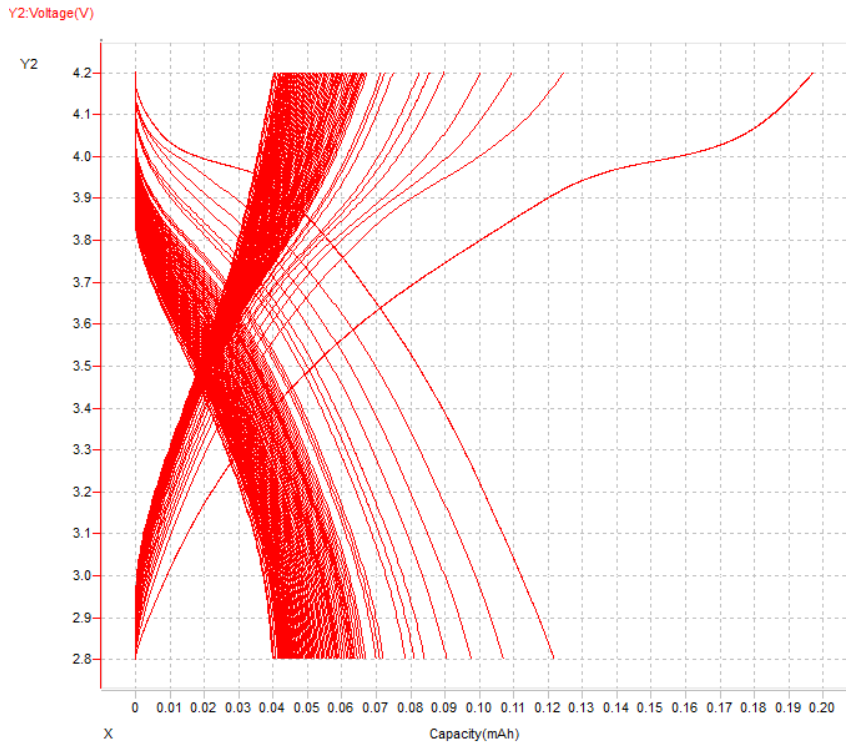

Figure 6.32 - Capacity vs Voltage profile, cell 4 without cycle 1

6.2.2 Charge and discharge specific capacity

In the first cycle of the as we can see in figures below, we have a peak of capacity maybe due to contamination. For example, in the first cycle of the cell 1 we have 0.34 efficiency so we lose the 66% and we will keep decrease in the next cycles. This loss can be due to LLI (Lithium Loss Inventory). The same behavior is present in the first cycle of all the cells analyzed.

Also, there are oscillations because of the night-day (temperature variations) shift but the main trend is good.

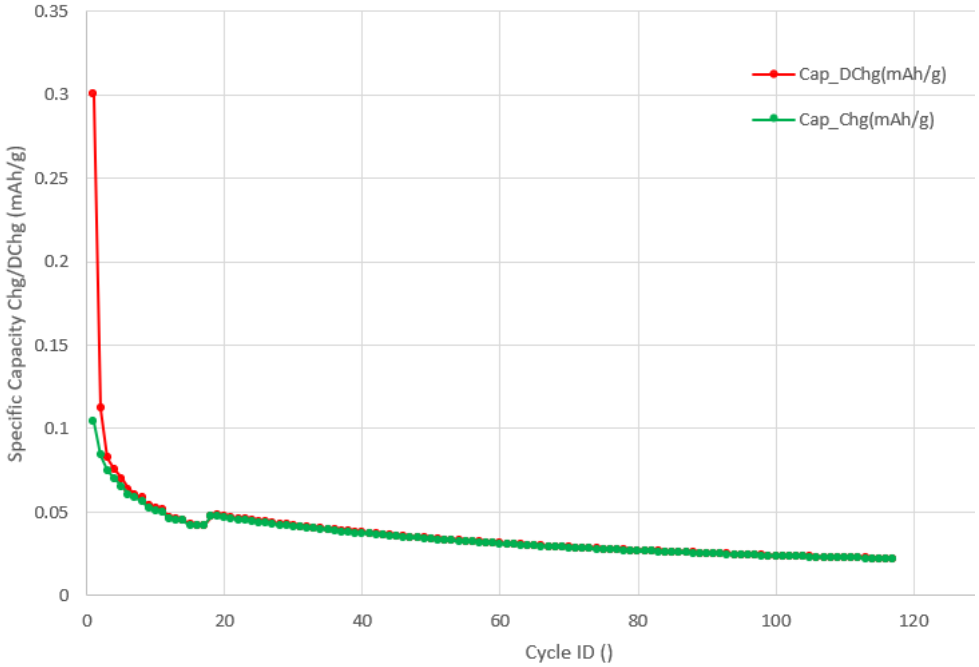

Figure 6.33 – Charge and Discharge specific capacity vs Cycle ID, cell 1

In cell 2, in the last cycle it's evident a sudden drop in capacity, from a normal behavior, directly to zero capacity. This probably is due to a disconnection of the battery while the last cycle was running.

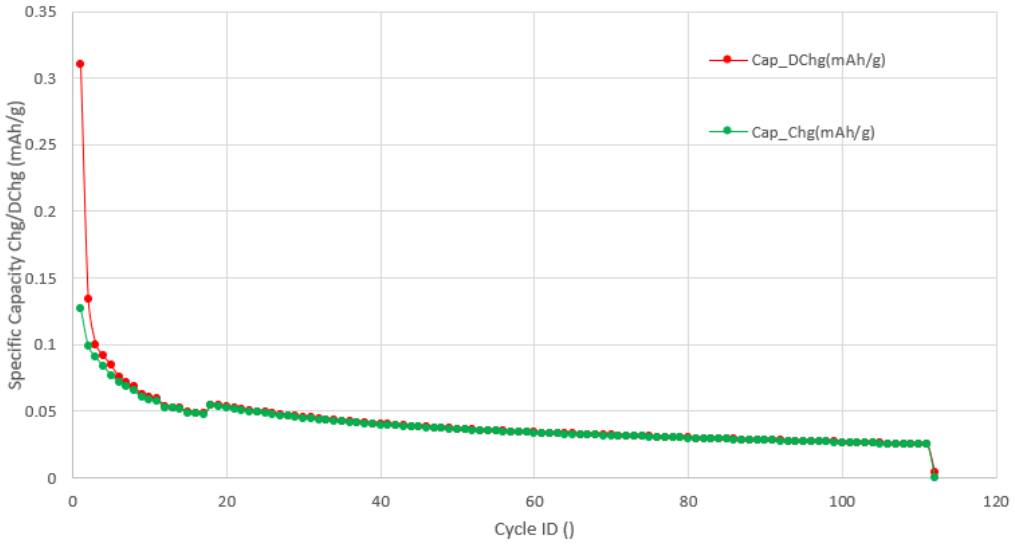

Figure 6.34 - Charge and Discharge specific capacity vs Cycle ID, cell 2

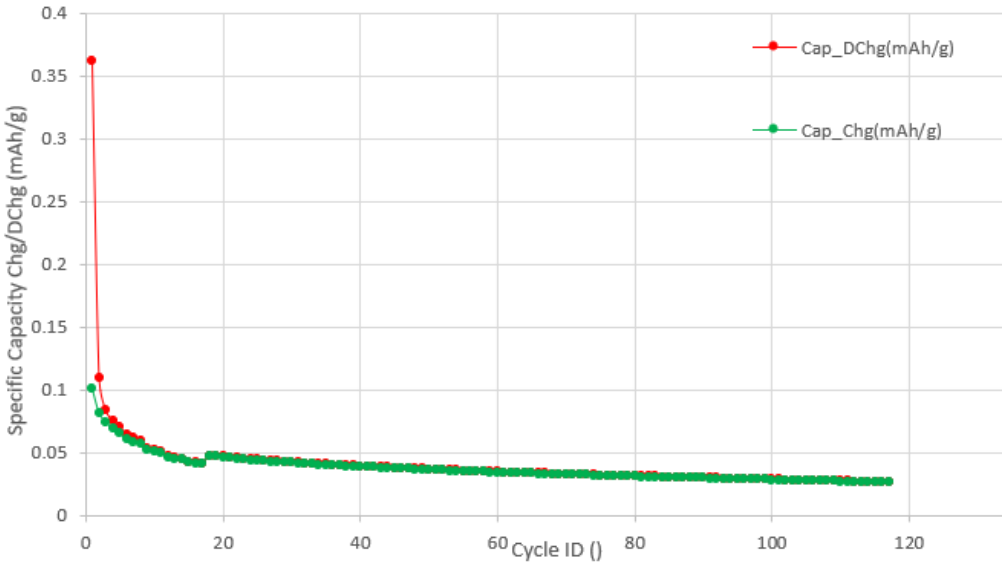

Figure 6.26 - Charge and Discharge specific capacity vs Cycle ID, cell 3

Also, in cell 4 as in 2, we can notice the decay in the last cycle. In addition, here the first cycle has a very low efficiency (16%) because we have a high difference between the specific capacity of charge and discharge.

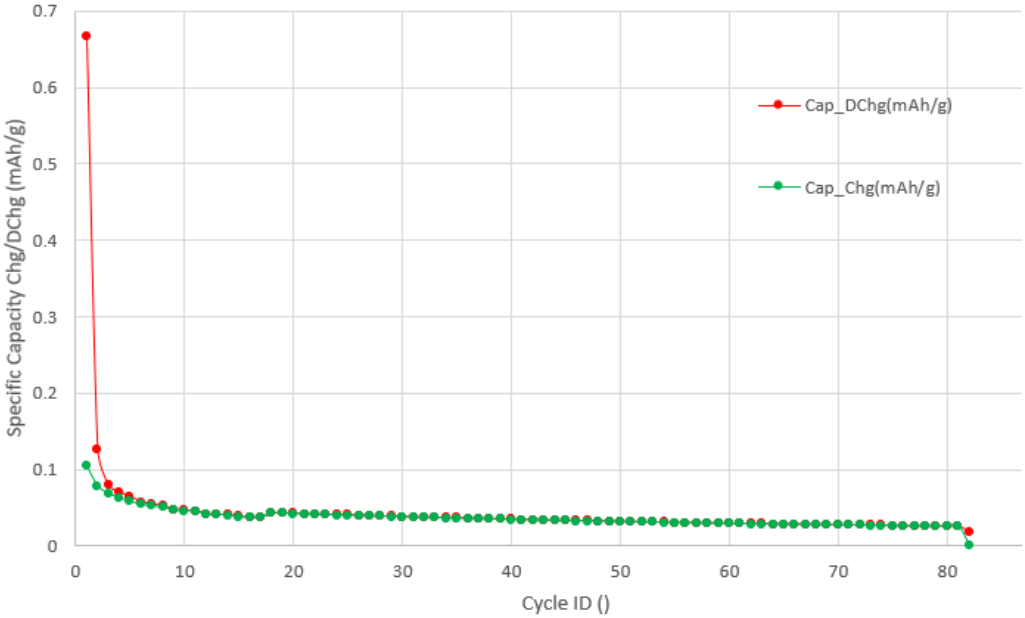

Figure 6.276 - Charge and Discharge specific capacity vs Cycle ID, cell 4

6.2.3 Coulombic efficiency

Analyzing the efficiency of the full cell we see that it is higher than that of half cells.

In cell 1 the efficiency after the cycle 20 stabilizes around 98.5% reaching 99% in the cycle 50 and then increases until it reaches 99.5%, while in cycle 18 reaches a value above 100%.

The behavior is the same in all the four cells which reaches values of efficiency higher than the half-cell case. A strange behavior is evident in cell 2 and cell 4 in the last cycle where there's a value of efficiency of 0, possibly due to the reason explained before.

A maximum coulombic efficiency of 99.557% was reached at the cycle 113 and finished with an efficiency of 99.531% at the cycle 117.

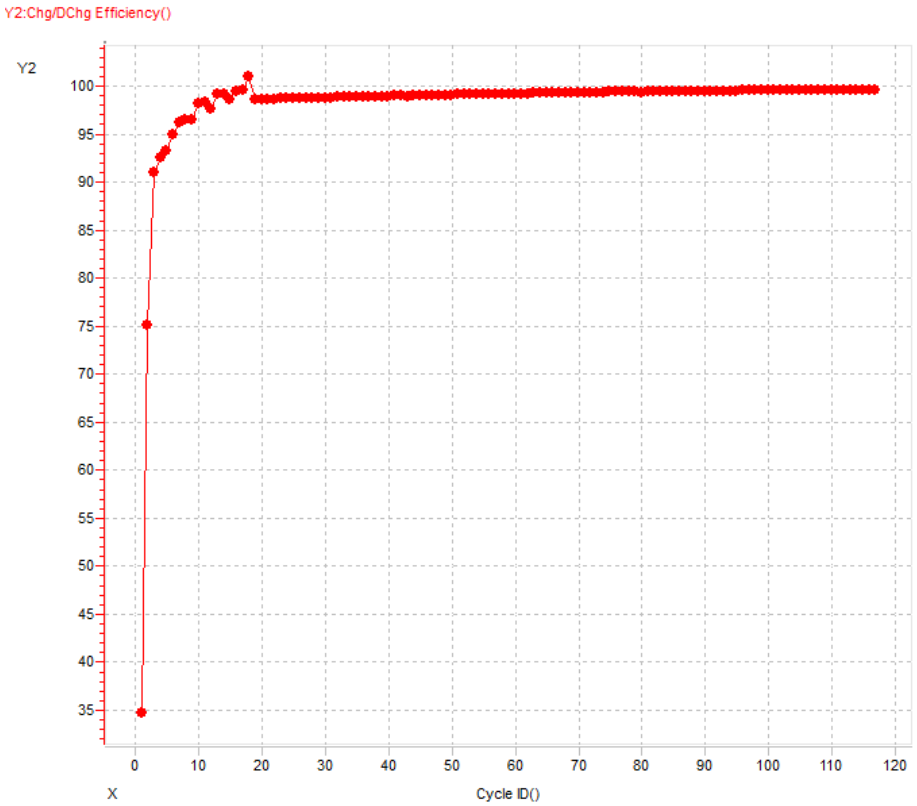

Figure 6.287 – Coulombic efficiency, cell 1

For cell 2, the maximum coulombic efficiency found was 99.640% and occurred in cycle 111 (one cycle before the last one). The test ended with cycle 112 with an apparent disconnection of the cell, and an efficiency of 0% for this reason.

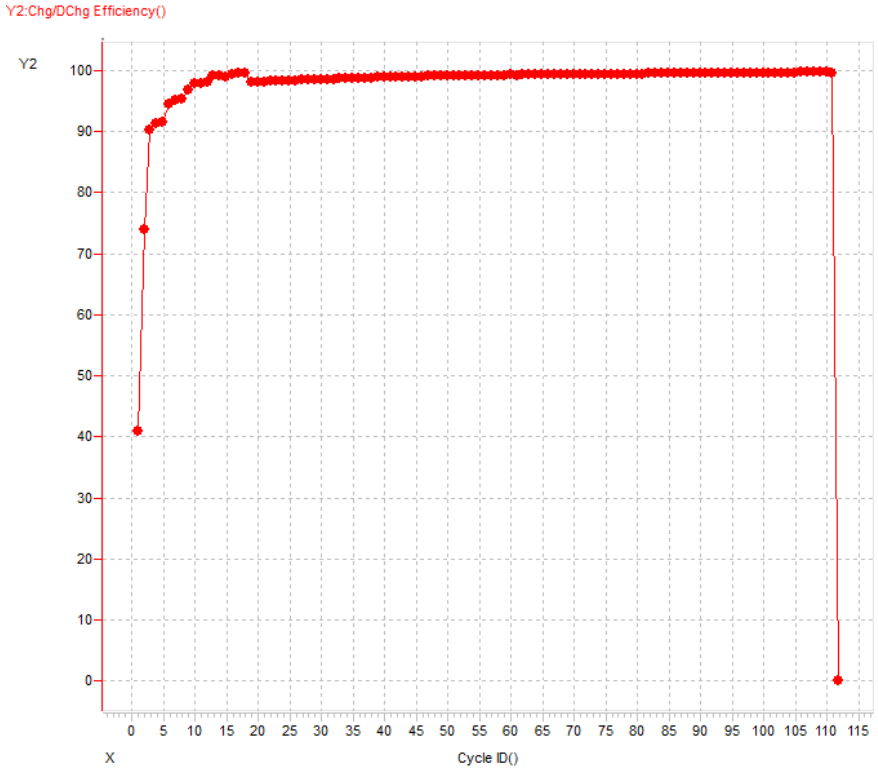

Figure 6.298 - Coulombic efficiency, cell 2

The cell 3 has reached a maximum coulombic efficiency of 99.282% at the cycle 98, and ended with a Coulombic efficiency of 99.056% at the last cycle 117.

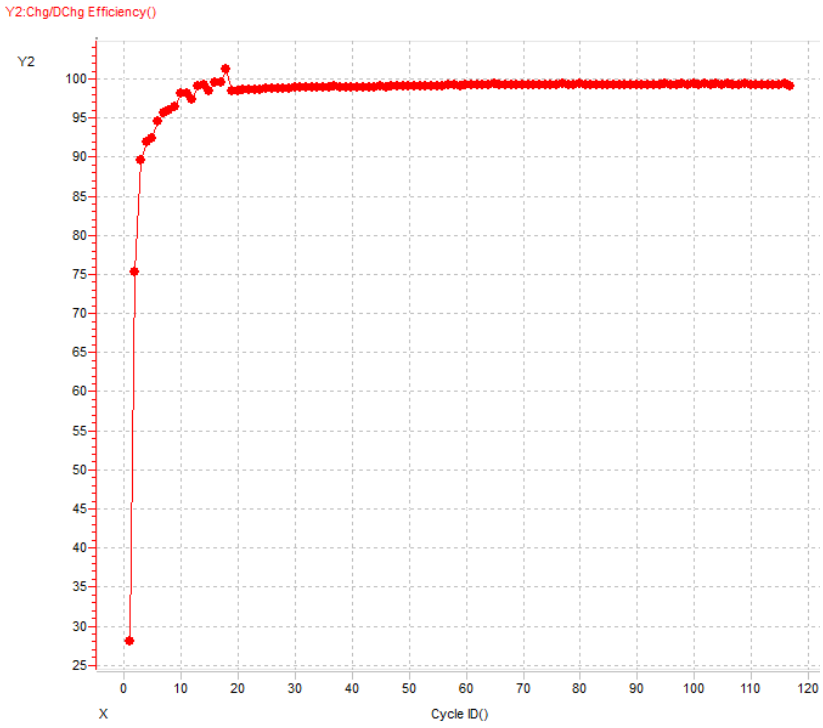

Figure 6.39 - Coulombic efficiency, cell 3

For cell 4, the maximum coulombic efficiency found was 99.078% and occurred in cycle 78. In the penultimate cycle (cycle 81) the efficiency was 98.931%.

The test ended with cycle 82 with an apparent disconnection of the cell, and an efficiency of 0% for this reason.

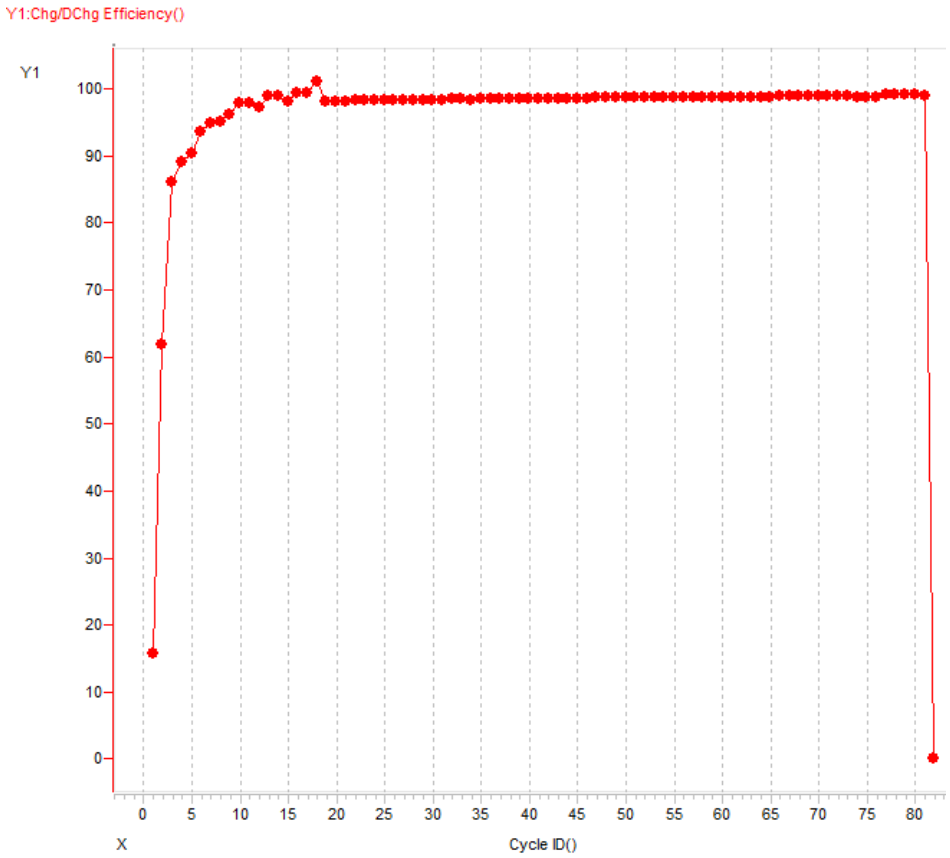

Figure 6.40 - Coulombic efficiency, cell 4

The best coulombic efficiency was found to be for the cell 2, for a maximum efficiency of 99.640%, while the cell 4 had the worst performance with an efficiency of 99.078%.

The result of this analysis is that the tested graphite electrodes perform better than the SiC ones in the charge reversibility. Having a high coulombic efficiency is fundamental to guarantee tong life of the cell, because even a lower efficiency of 99% means that with each cycle, 1% of the stored capacity is being used over and over in unreversible reactions that remove active material from the redox reaction of interest.

6.2.4 Capacity fading analysis

We examined the cycles required to achieve 80% of the maximum specific capacity in all fully charged cells. The observed fluctuations are likely attributed to uncontrolled temperature variations during the analysis. The first figure shows the specific capacity in the first cycle where the values of

the Crate is changing than the second figure represents the capacity fading analysis keeping the Crate constant equal to 1.

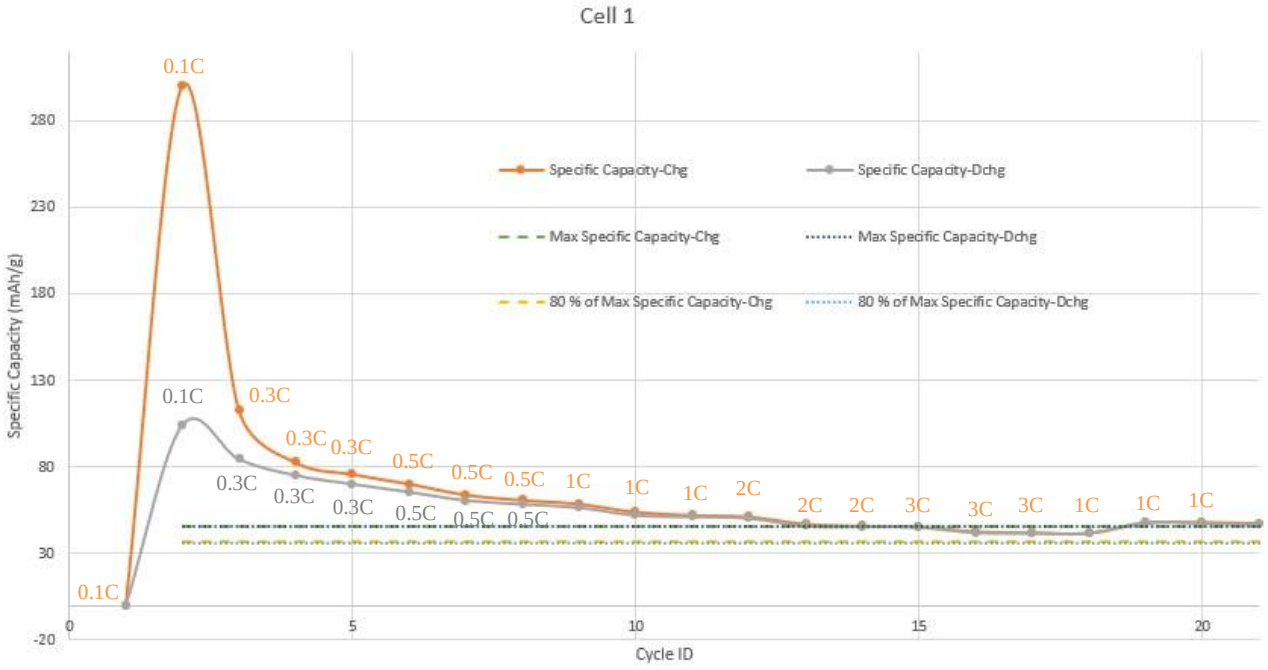

The first cycle as an evident problem because the specific capacity reach a very low value, then we have a very steep decrease from cycle 2(mAh/g) to cycle 3(mAh/g). The values of specific capacity of charging and discharging are quite identical after the cycle 5 due to the high efficiency. The valu of the specific capacity decreases very sharply from cycle 2 to cycle 10 due to the increase of the Crate from 0.1C to 1C. In the Crate costant analysis is evident a steep decrease of the specific capacity charging and discharging which seems to be very similar to each other due to the high efficiency in the last cycles. The 80% of max capacity is reached after 43 cycles.

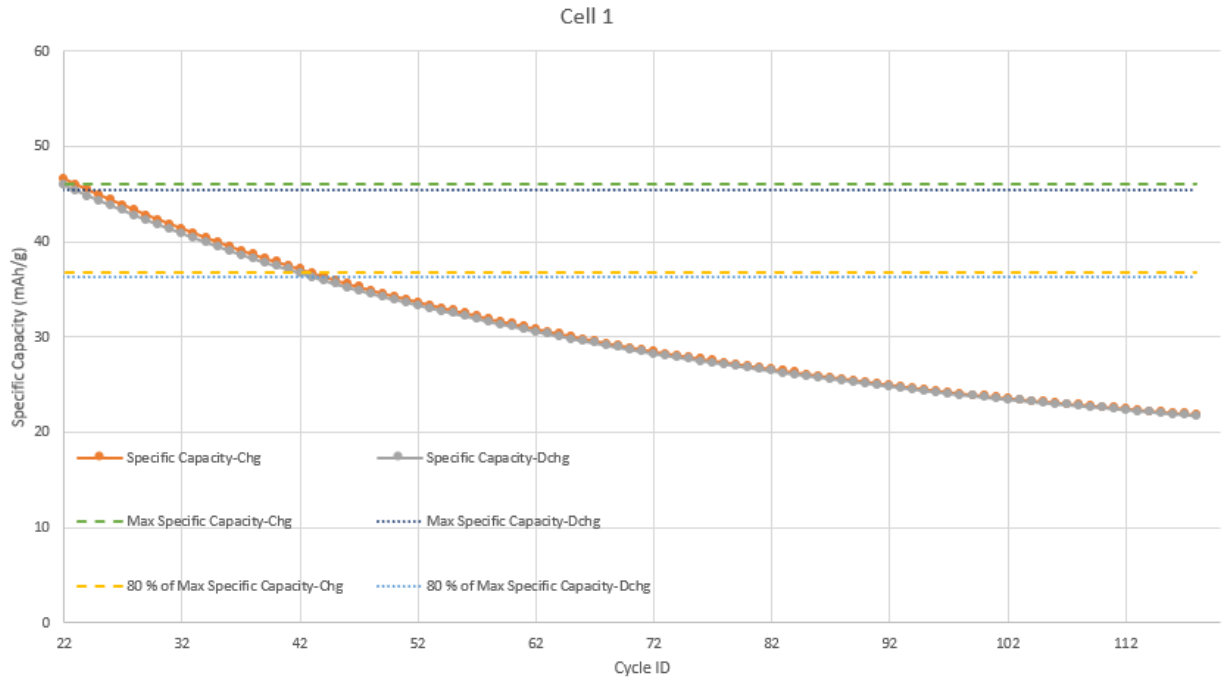

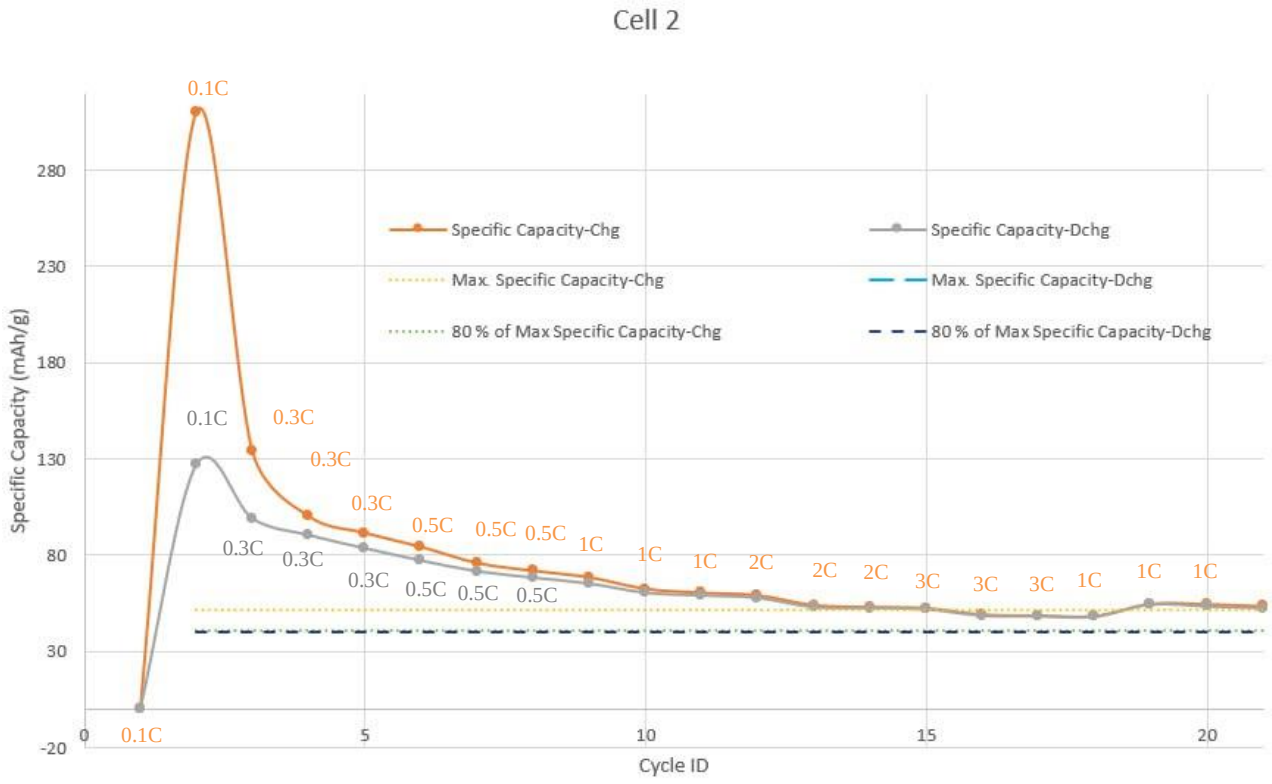

The behavior of cell 2 is very similar to the cell 1 with a very high different from cycle 2 and cycle 3. There are sligthly varitiond between the cycles varying the Crate, for example there is a steep

change between the cycle 9(mAh/g) to cycle 10(mAh/g). There's a sharp increse of specific capacity between cycle 18(mAh/g) and cycle 19(mAh/g).

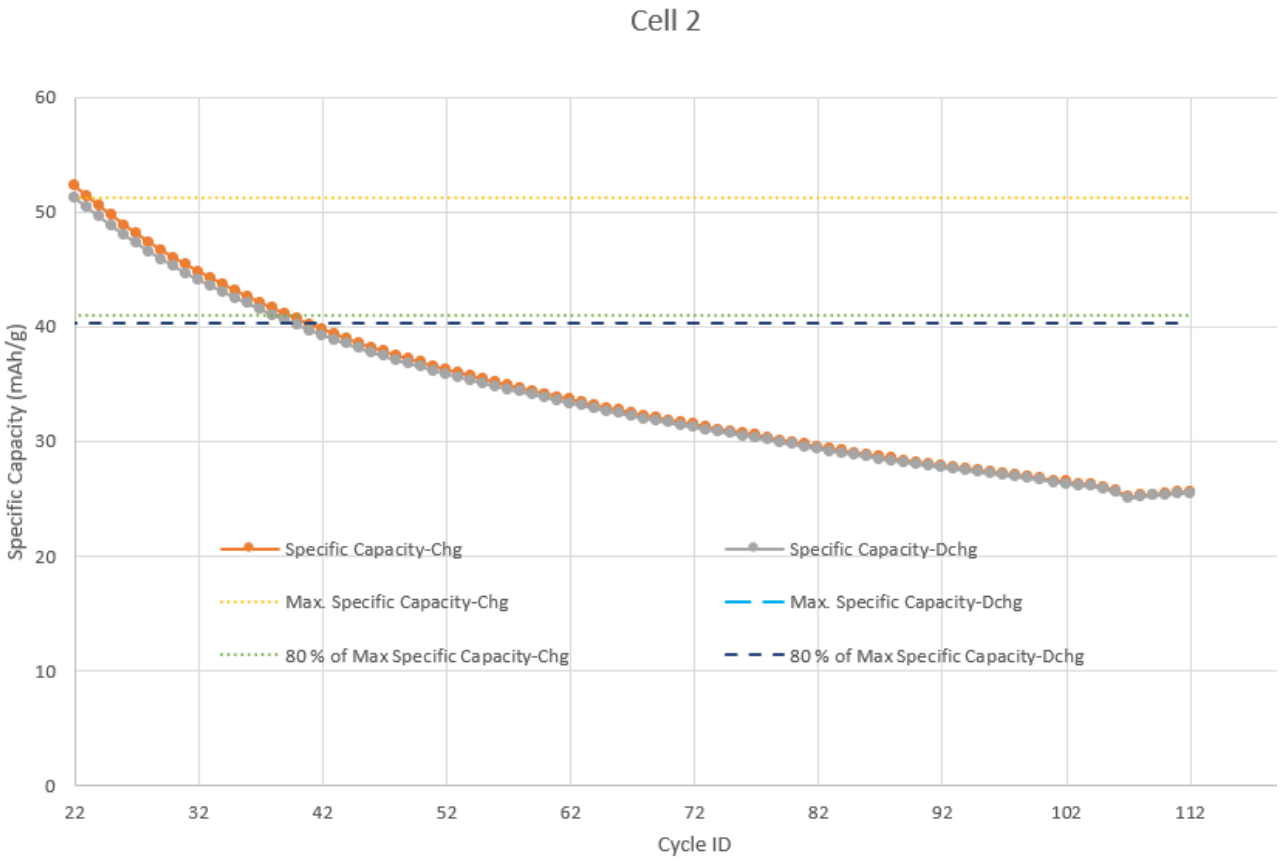

The analysis at constant Crate is very similar to the cell 1 so we can see the same behavior. There's a strange decrease around cycle (quale è ciclo dove ce la capacita piu bassa dopo il 102 ?). The 80% of maximum capacity is reached after 39 cycles.

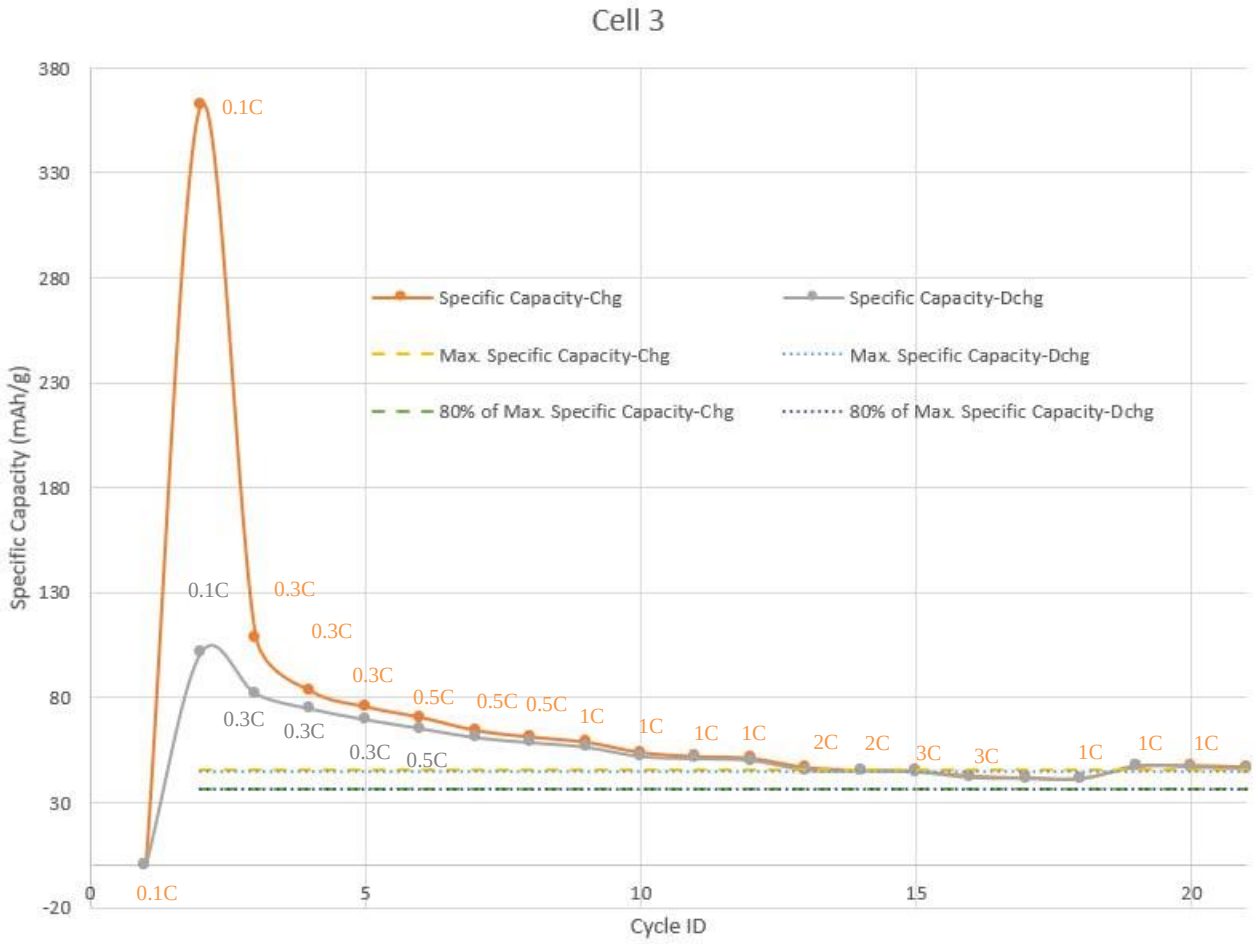

The behavior of cell 3 is identical to the cell 2 in the cycle varying the Crate. The behavior after making the Crate constant is very similar to the other 2 cells before but it reaches the 80% of maximum capacity after them at cycle 50.

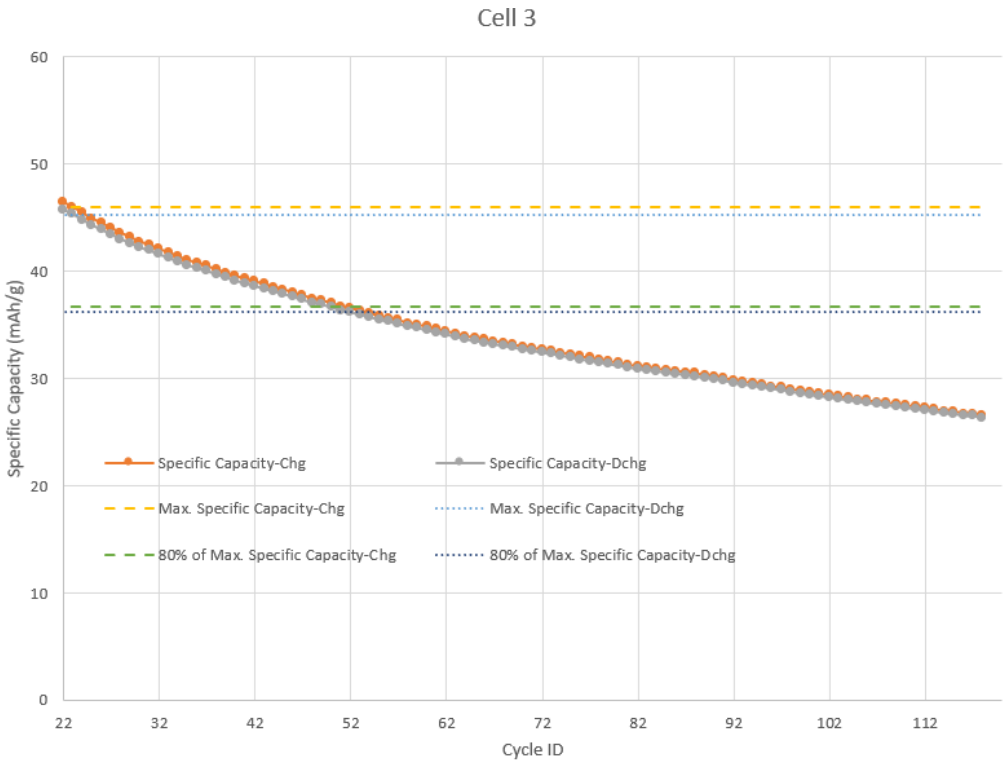

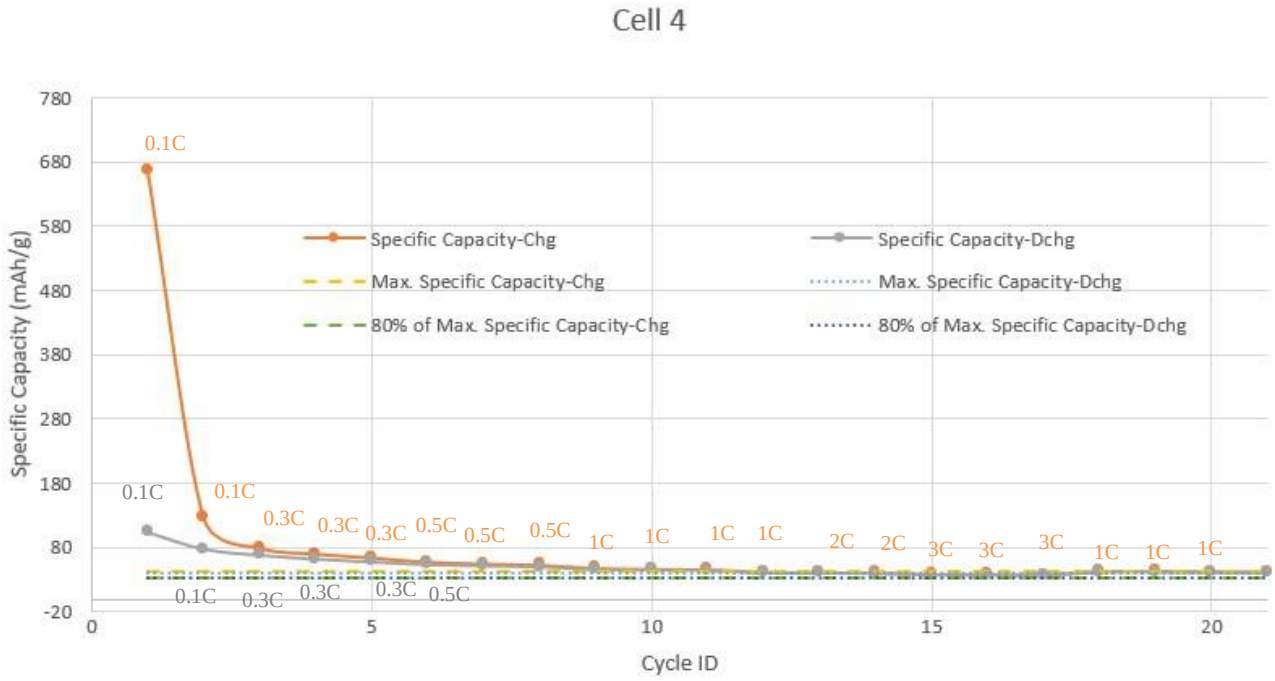

The cell 4 has a different behavior because the first cycle have a much higher specific capacity and the steeper part is from cycle 1(mAh/g) to cycle 2(mAh/g). The value of specific capacity charging and discharging have a plateau from cycle 5 so the variation of Crate seems too be not so evident in this cell.

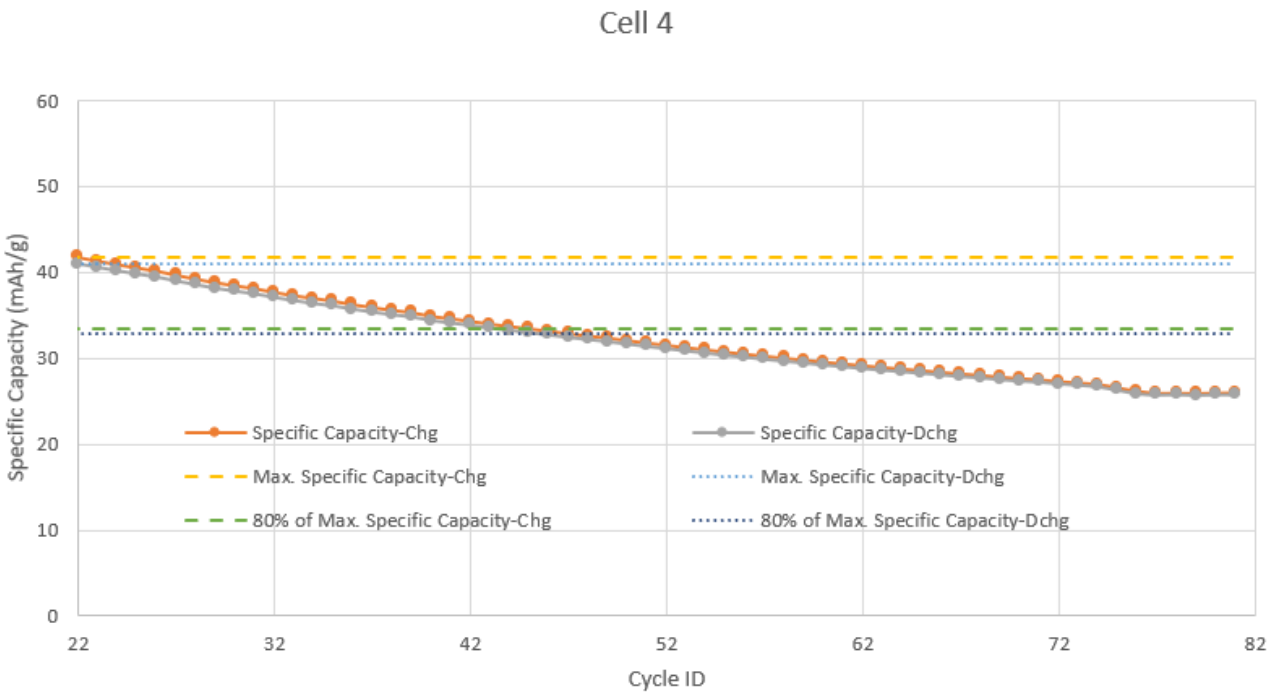

Figure 6.41 - Charge and Discharge specific capacity fading

The cell 4 has different behavior also in the constant Crate analysis because the decrease is slighter and the trend is almost horizontal. The cell 4 reaches the 80% of maximum capacity at cycle 46.

The outcomes are rather discouraging as the 80% threshold is attained within the already initial 25 cycles, followed by a noticeable decline. However, there is an increase in both cells due to the C-rate changing, indicating satisfactory performance as happened in the half cell analyisis. The table below presents the results of capacity fading:

Cell Number	Max.Specific-Chg Cycle ID	80% of Max. Specific-Chg Cycle ID	Number of Cycle	Max.Specific-Dchg Cycle ID	80% of Max.Specific-Dchg Cycle ID	Number of Cycle
Cell 1	22	42	20	22	43	21
Cell 2	22	39	17	22	39	17
Cell 3	22	50	28	22	51	29
Cell 4	22	46	24	22	46	24

7. Conclusions

At the end of our analysis, we can affirm that the results are satisfying, and they are very close to the expected one. The repeatability of our analysis has been useful to find the cells which behavior is acceptable. In fact, some of our samples had problems and have been useless for our analysis. The limited number of cycles and samples doesn't allow us to understand the causes of some phenomena because we don't have enough data. The experimental campaign occurred without major incidents and all the samples have been managed carefully and in a protected environment. Better results can be reached with more accurate measurements and procedures and adding samples to our analysis. An example of inaccuracy can be found in the value of active material in the half cell analysis because the software didn't allow us to be precise and use further significant figures. Other issues which led to inaccuracies may have happened in the assembling phase when the components were not properly aligned. As we can see in the analysis of cell 4 and 7, the results have been problematic due to problems of connection, conditions of the cells and software. The same problems can be the cause of

the efficiency drop of the full cell 2and 4 in the last cycle. The results of the full cell analysis allow us to affirm that the cells using graphite had a better cyclability than the SiC cells which is evident in the coulombic efficiency analysis.

8. References

1. **Aot.** https://www.aotbattery.com/. [Online]

2. ***Gate, Research.***

3. ***Neware since 1998.*** *[Online]*

4. Stabilizing Capacity Retention in NMC811/Graphite Full Cells via TMSPi Electrolyte Additives. ***Josefa Vidal Laveda, Jia En Low, Francesco Pagani, Evelyn Stilp, Stefan Dilger, Volodymyr Baran, Michael Heere, and Corsin Battaglia.*** *2019.*

5. Structural degradation of graphite anode induced by dissolved manganese. ***Hosop Shin, Yoon Koo Lee, Wei Lu.*** *2022.*

6. Layered silicon carbide: a novel anode material for lithium ion batteries. ***Abdul Majid, Afrinish Fatima, Salah Ud-Din Khanb and Shaukat Khanc.*** *2021.*